ADVANCED TECHNOLOGY LABORATORIES

N63 18493

ₗₒₚₑ₋ᵢ

DESIGN CRITERIA FOR ZERO-LEAKAGE CONNECTORS FOR LAUNCH VEHICLES. VOL. 2, LEAKAGE FLOW

Edited by

T.P. GOODMAN

GENERAL ⊛ ELECTRIC

FINAL REPORT FOR FIRST CONTRACT PERIOD

(March 1962 through February 1963)

DESIGN CRITERIA

FOR ZERO-LEAKAGE CONNECTORS

FOR LAUNCH VEHICLES

Contract NAS 8-4012

VOLUME 2

LEAKAGE FLOW

Edited by T.P. Goodman

March 15, 1963

CONTENTS

21. STANDARDS FOR "ZERO LEAKAGE"

by

T. P. Goodman

21.0 Summary

"Zero leakage" has a much more stringent meaning in rocket propulsion systems than in the more conventional technologies such as steam-power-plant design. In a rocket propulsion system, it is not sufficient simply to have "stable leakage" or "leakage by molecular diffusion only". In rocket systems, zero leakage as determined from a bubble test means leak rates less than 10^{-4} atm cc/sec. or 10^{-6} lb. of air per hour; however, laboratory measurements with mass-spectrometer leak detectors can detect leaks of one-millionth of this magnitude. Leakage by diffusion through solid walls is generally well below zero leakage as determined by a bubble test, though still readily detectable by mass-spectrometer measurements.

4

21.1 Introduction

The development of rocket propulsion systems imposes requirements of hitherto unknown severity on the leak-tightness of fluid connectors. Until recently, most of the technology of fluid connectors was developed for fluids such as steam, for which leak-tightness was primarily a matter of the cost of the escaping fluid. In rocket systems, the leakage of fuels and oxidizing agents can cause explosions. Moreover, when fuels are stored in space satellites for later use in returning to earth, leakage must be reduced to an absolute minimum to economize on the payload of the satellite and to increase reliability of operation.

There are two traditional interpretations of "zero leakage" which are useful for steam power plants but are wholly inadequate for rocket propulsion systems. The first interpretation of "zero leakage" might better be called "stable leakage". Roberts (Ref. 1) has shown that a gasketed flange joint having uniform gasket pressure is theoretically stable when the ratio

$$m = \text{gasket pressure/internal pressure}$$

is greater than 1, and unstable when m is less than 1. When m 1, the internal pressure tends to blow the joint apart. In practice, some joints are found to be stable when when m 1, but Roberts attributes this to sticking of the gaskets. In a stable joint, there is still a small amount of leakage between the gasket and flange surfaces, but in steam-power-plant practice this stable leakage is often interpreted as "zero-leakage" because the cost of the steam that escapes is negligible. In a rocket propulsion system, even this leakage through a "stable" leak can be unacceptable.

A second interpretation of "zero leakage" might better be called "leakage by molecular diffusion only". Flow through a large passage under large pressure differential is generally turbulent; as the passage size decreases, flow becomes laminar. When the clearance in the passage is decreased to the same order of magnitude as the mean free path of the fluid molecules, the laminar flow changes to a flow by molecular diffusion. When the passage clearance is so small that flow is by molecular diffusion, the resulting flow is often thought of as "zero leakage"; however, even the small flow by molecular diffusion may be too much for a rocket propulsion system. Indeed, as shown in Section 22 of this report, the rate of molecular diffusion flow through a given passage is greater than the rate of laminar flow would be through the same passage.

5

21.2 Quantitative Measurements

For rocket propulsion systems, since both the "stable leakage" criterion and the "leakage by diffusion only" criterion are inadequate, it is important to specify quantitatively the leakage that is acceptable in a given connector. Then appropriate measurement techniques must be used to determine whether this leak-tightness has been achieved. Some highly accurate means are available for laboratory measurement of leak-tightness, but unfortunately, field measurement techniques are much less precise. Nevertheless, the laboratory measurements can be employed to evaluate new design principles.

To obtain an idea of the order of magnitude of leakage required in rocket launch vehicles, we have attempted to arrive at a quantitative working definition of "zero leakage." From our discussions in Huntsville we concluded that a good working definition of "zero leakage" is a leakage rate such that no bubbles can be detected in half an hour when a fully pressurized connector is immersed in water. Information obtained from the ATL Vacuum Center indicates that the threshold leakage rate at which no bubbles would appear in 5 to 15 minutes is approximately 2×10^{-6} lb/hr of air at room temperature and atmospheric pressure. Thus, for no bubbles in half an hour, the threshold flow rate may be taken as 10^{-6} lb/hr of air at standard conditions. For this flow rate, a single bubble appearing every half hour would have a mass of 0.5×10^{-6} lb and a diameter of 0.28 in. at standard conditions. Since some air would dissolve in the water rather than appearing in bubbles, the bubbles for this leak rate would actually be somewhat smaller. Thus, 10^{-6} lb/hr appears to be a reasonable definition of "zero leakage" as detectable from a conventional bubble test.

Table 21.1 compares the leakage rates that can be discerned from a conventional bubble test with leak rates that are discernible by other measurement techniques. Since many different units are used in describing leakage rates, all the measurements are shown in several different systems of units. It is convenient to remember that for air, 1 lb/hr is very nearly equal to 100 atm cc/sec. An "atm cc" (atmospheric cubic centimeter) is the mass of fluid that would occupy a volume of one cubic centimeter at room temperature and atmospheric pressure. A "micron-ft^3" is the mass of fluid that would occupy a volume of one cubic foot at a pressure of one micron of mercury (1/760,000 atmosphere) at room temperature.

From Table 21.1 it can be seen that by standard mass-spectrometer flow measurements, flows in the "zero leakage" range can be quantitatively evaluated with high precision. The mass spectrometer was used to make the flow measurements described in Volume 3 of this report.

6

TABLE 21.1 SENSITIVITIES OF LEAK-MEASURING METHODS

Type of Measurement	Application	Volume of Helium or Air			Mass Flow (Air)
		$\frac{\text{Micron-ft.}^3}{\text{hr.}}$	$\frac{\text{atm-cc}}{\text{sec.}}$	$\frac{\text{atm-ft.}^3}{\text{hr.}}$	$\frac{\text{lb.}}{\text{hr.}}$
A. Bubble test (immerse fully pressurized connector in fluid and look for bubbles)	Component test				
1. Using water at room temperature and atmospheric pressure.					
a. No bubbles in 5 to 15 min. (Ref. 2)		20	2.08×10^{-4}	2.64×10^{-5}	2.02×10^{-6}
b. No bubbles in 30 min. (estimated)		10	1.04×10^{-4}	1.32×10^{-5}	1.01×10^{-6}
2. Using water at room temperature with pressure above bath reduced to 2 in. Hg(= above 0.07 atmosphere) (Ref. 3).		3	3.12×10^{-5}	3.96×10^{-6}	3.03×10^{-7}
3. Using silicone oil (Ref. 3)					
a. At 150°C and atmospheric pressure		0.45	4.61×10^{-6}	5.85×10^{-7}	4.49×10^{-8}
b. At room temperature with pressure above bath reduced to 1.5 in. Hg (= about 0.05 atmosphere)		0.056	5.85×10^{-7}	7.43×10^{-8}	5.69×10^{-9}
B. Displacement of water in burette by leaking gas	Component test	1.6	1.67×10^{-5}	2.12×10^{-6}	1.62×10^{-7}
C. Soap-bubble test (apply soap solution around connector and look for bubbles) (Ref. 2)	Field Assembly Test	5	5.2×10^{-5}	6.6×10^{-6}	5.0×10^{-7}
D. Mass spectrometer leak detector (Refs. 3, 4)*	Laboratory Test				
1. With maximum sensitivity		0.96×10^{-6}	1×10^{-10}	1.27×10^{-11}	0.97×10^{-12}
2. With lower sensitivity		0.96×10^{-5}	1×10^{-9}	1.27×10^{-10}	0.97×10^{-11}

*Mass spectrometer detects flow of helium. In laminar flow, volume flow of helium = volume flow of air for the same leak under the same pressure and temperature conditions, since viscosities of air and helium are approximately the same. In molecular flow, volume flow of helium ≈3x volume flow of air for the same leak under the same pressure and temperature conditions. See section 22.

7

21.3 References

1. I. Roberts, "Gaskets and Bolted Joints", *Trans. ASME, J. Appl. Mech.*, Vol. 17, 1950, pp. 169-179.

2. R. A. Koehler, GEL Internal Memorandum on Vacuum and Pressure Testing, 1953.

3. H. S. Scheffler, *Final Report on Task 511, Leak Detection*, Battelle Memorial Institute, 1959.

4. General Electric Co., *Instruction Book for Type M-60 Mass Spectrometer Leak Detector.*

8

22. FLOW CALCULATIONS FOR SMALL PASSAGES

by

B.T. Fang and P.N. Le Fort

22.0 Summary

An analysis of a one-dimensional channel flow model of leakage is developed and leakage flow calculations are made for the gases:

1. helium
2. hydrogen
3. oxygen
4. nitrogen

and for the liquids:

1. hydrogen
2. oxygen
3. RP-1

for pressures up to 1000 atmospheres and clearances up to 200 microinches.

The results are plotted as graphs for a representative flow passage. Equations are given for converting the results to flow passages of other dimensions.

9

22.1 Introduction

Since it is impossible to obtain perfectly smooth surfaces, there will be minute clearances between the two surfaces of flanged connectors. Fluid under pressure will tend to seek its way through these small clearances. For a certain fluid at a given pressure and temperature, the amount of leakage depends on the geometry of the clearance. As a first step toward the understanding of the leakage process, we shall replace the actual situation of leaking through the many small irregular passages by a model of one-dimensional flow through a channel of length ℓ, width w and thickness h. In the simplest representation we can take

ℓ = width of flange (in the direction of leakage flow)

w = mean perimeter of flange

h = clearance between flanges

A more sophisticated approach is to take ℓ, w, h as some kind of statistical averages of the geometry, surface finish and clamping pressure of the flanges. The proper selection of these values for a given fluid connector will be the subject of Section 33. The purpose of the present section is to determine the amount of leakage when the dimensions ℓ, w, h of the passage are known and to present values for the flow of various gases and liquids through a passage of typical size.

10

22.2 Parameters Defining Flow Regions

The leakage may have the character of turbulent flow, laminar flow, or molecular flow. Roughly speaking, turbulent flow occurs at the highest rate of leakage and molecular flow occurs when the leakage rate is very small. Since we are primarily interested in achieving a very small amount of leakage, the leakage process will generally be in the laminar-flow and molecular-flow regions.

The parameter which defines the laminar and turbulent flow regions is the Reynolds number $\frac{\rho vh}{\mu}$

where

$$\rho = \text{density of fluid}$$

$$v = \text{velocity of fluid}$$

$$\mu = \text{viscosity of fluid}$$

For a cylindrical tube (h = diameter, d) the critical Reynolds number is about 2000, beyond which turbulent flow may occur. For a channel, the critical Reynolds number will be somewhat smaller. A good estimate is to take the critical Reynolds number as 2000 based on an equivalent diameter (Ref.9) defined as

$$d = 4 \times \frac{\text{Cross Sectional area of Channel}}{\text{Perimeter of channel}}$$

$$\cong \frac{4 \ wh}{2 \ w} = 2 \ h$$

This would give us a critical Reynolds number of 1000 based on the clearance h.

Notice that for steady isothermal channel flow the Reynolds number is approximately constant throughout the length of channel. This means that it is very unlikely that part of flow in the channel is laminar while the rest is turbulent.

The parameter which defines the laminar and molecular flow regions is the Knudson number λ/h, where λ is the mean free path of the gas molecules. Molecular flow dominates when the mean free path is of at least the same order of magnitude as the thickness i.e., when the Knudson number is of the order of 1 or greater. Since the mean free path is inversely proportional to the pressure at a given temperature, Knudson's number increases in the direction of flow. It often happens that at the entrance of the channel the flow is laminar while at the exit it becomes molecular.

11

22.3 Rate of Leakage in Laminar Flow

The equations which govern the flow rate are

(1) Conservation of mass

(2) Momentum equation

(3) Energy equation

In steady flow, conservation of mass requires the mass flow rate across any cross section of channel to be a constant. The energy equation comes in when the flow is compressible. The momentum equation is from the well known Navier-Stokes equations which assume a simple form for one-dimensional channel flow.

In our application the flow velocity is small so that

(1) Inertia effect can be neglected   (Section 22.9.2)

(2) Normal viscous stress can be neglected

(3) Turbulence does not occur.

Under these conditions the pressure gradient which causes the flow is balanced by the retarding viscous friction at the walls of the channel. It is well known that the velocity profile across the channel is parabolic (the consideration of entrance length is given in Section 22.9.1) and that the mass rate of flow is

$$Q = - \frac{\rho dP}{dx} \frac{wh^3}{12\mu} \qquad (1)$$

where $- \frac{dP}{dx}$ = pressure gradient in the direction of flow

ρ = density of fluid

μ = viscosity of fluid

For incompressible fluids such as liquids, Eq.(1) can be integrated, assuming ρ and μ are not pressure dependant, to give

$$Q = \frac{\rho \, wh^3 \, \Delta P}{12\mu\ell} \qquad (2)$$

where ΔP = pressure difference

For compressible gases, thermal effects come into play and Eq.(1) cannot be integrated directly. Since the flow is very slow and the thickness of channel very small, the flow is approximately under isothermal conditions (Section 22.9.2). For a gas behaving essentially as a perfect gas Eq. (1) can be integrated to give.

12

$$Q = \frac{wh^3 (\triangle P) \ \bar{P}}{12 \ \mu \ell \ P/\rho} = \frac{m \ wh^3 (\triangle P) \ \bar{P}}{12 \ RT \ \mu \ell} \qquad (3)$$

where

$\bar{P}$ = mean pressure

T = absolute temperature

R = universal gas constant

m = molecular weight

It is readily seen from Eq. (2) and (3) that for both gases and liquids the mass rate of leakage is

(1) Proportional to

(a) Width of channel

(b) Cube of thickness of channel

(2) Inversely proportional to

(a) Viscosity of fluid

(b) Length of channel

For liquids the rate of leakage is further proportional to the pressure difference and to the density of liquid. For gases the rate of leakage is proportional to the pressure difference and to the mean pressure. For large pressures it is therefore approximately proportional to the square of internal pressure. The leakage rate is also inversely proportional to the absolute temperature and directly proportional to the molecular weight of the gas. It is evident that in the leakage of either liquids or gases the most effective means of reducing leakage is to decrease the clearance between the flanges.

13

22.4. Molecular Flow Correction

In order to achieve a very small leakage rate, the clearance between sealing surfaces has to be very small. When the clearance becomes so small that it is of the same order of magnitude as the mean free path of the gas molecules, leakage by the process of random molecular motion becomes of importance. The essential correction is that the no-slip condition at the channel walls is no longer true. Therefore, the leakage rate will be greater than that computed from the laminar-flow equation.

Knudson proposed the following formula for the leakage rate in free molecular flow (Ref.1,2):

$$\frac{4V_a \rho (\Delta P)/P}{3\int_0^{\ell} (H/A^2) \, d\ell} \tag{4}$$

where

      H = perimeter of channel

      A = cross section of channel

      ℓ = length of channel

      V_a = mean molecular speed = $\sqrt{8 \, RT/\pi m}$

This equation can also be rewritten as

$$Q = \frac{8\sqrt{2} \, (\Delta P)}{3\sqrt{\pi RT/m} \int_0^{\ell} (H/A^2) \, d\ell} \tag{5}$$

which shows that the leakage rate is

    (1)   proportional to the pressure difference.

    (2)   inversely proportional to the square root of absolute temperature.

    (3)   proportional to the square root of the molecular weight of the gas.

The effect of geometry of the channel on the leakage rate is represented by the factor

$$\int_0^{\ell} (H/A^2) \, d\ell$$

which shows that

    (1)   For the same channel cross sectional area, the greater the perimeter-to-area ratio, the smaller the amount of leakage. Therefore, the circular tube is the least desirable shape.

11

(2) For a channel of given shape (H/A = constant) but changing cross-sectional area, the smaller cross sections have a choking effect on the amount of flow. For instance, a channel of changing cross section allows less flow than a constant-area channel having the same cross-sectional area as the mean cross-sectional area of the changing channel.

It is convenient to put the leakage-rate equation into yet another form. From kinetic theory of gases we have the mean free path of gas molecules as

$$\lambda \cong 2(\mu/P) \sqrt{RT/m} \qquad (6)$$

Substituting in the leakage-rate equation, we have

$$Q = \frac{4}{3}\sqrt{\frac{2}{\pi}} \frac{1}{\int_{o}^{\ell} H/A^2 \, d\ell} \frac{\rho}{\mu} \bar{\lambda}\bar{P} \frac{\Delta P}{P} \qquad (7)$$

where $\bar{\lambda}$ is measured at the mean pressure .

For the rectangular channel we have been considering, the above formula becomes

$$Q = \frac{2}{3}\sqrt{\frac{2}{\pi}} \frac{\rho \, wh^2}{\mu \, \ell} \bar{\lambda}\bar{P} \frac{\Delta P}{P} \qquad (8)$$

If we compare this with the leakage rate as computed from the laminar flow equation (3), we obtain

$$\frac{Q \text{ free molecular flow}}{Q \text{ laminar flow}} = 8\sqrt{\frac{2}{\pi}} \frac{\bar{\lambda}}{h}$$

$$= 8\sqrt{\frac{2}{\pi}} \times \text{(Knudson's number)} \qquad (9)$$

which also shows that Knudson's number is our measure of whether the flow would be essentially laminar or molecular.

Strictly speaking, Knudson's equation applies only to free molecular flow where the mean free path is very large compared to the clearance h. For transition flows the following modified equation has been proposed (Ref.2).

$$Q = Q_{\text{laminar flow}} + \epsilon Q_{\text{free molecular flow}}$$

where ϵ is of the order of magnitude unity. The exact value of ϵ depends on the gas and properties of passage walls. For a capillary tube Adazumi (Ref.3) showed that

$$\epsilon \cong 0.9 \quad \text{for a single gas}$$

$$\epsilon \cong 0.66 \text{ for gaseous mixtures such as air}$$

15

We shall base our calculations on these values, which should give us a correct order of magnitude of the leakage rate. We have shown (Eq. 9) that it is possible to express $Q_{free\ molecular\ flow}$ in terms of $Q_{laminar\ flow}$ and Knudson's number. Therefore, it is convenient to write the total leakage rate as $Q_{laminar}$ times a correction factor. Thus for a circular cross-section

$$Q = Q_{laminar}\left(1 + \epsilon \frac{16}{3}\sqrt{\frac{2}{\pi}}\ \frac{\bar{\lambda}}{r}\right) \tag{10}$$

and for the rectangular channel we have been considering

$$Q = Q_{laminar}\left(1 + \epsilon\ 8\sqrt{\frac{2}{\pi}}\ \frac{\bar{\lambda}}{h}\right) \tag{11}$$

The second term in the parenthesis represents the molecular flow correction factor.

We shall illustrate the result with a few numerical examples.

Consider the leakage of air at 60°F from a pressure of 24.5 atm. to the atmosphere. The leaking passage has length ℓ = 0.1 in., width w = 5 in. and clearance 1 microinch. The laminar-flow equation would give us a leakage rate of

$$Q_{laminar} = 10^{-6}\ lb/hr$$

For air at 60°F and atmospheric pressure the mean free path is 3.5 micro-inches. At a mean pressure of (24.5 + 1)/2 = 12.75 atm., the mean free path is

$$\bar{\lambda} = 3.5/12.75 = 0.27\ microinch$$

The molecular correction factor is

$$(.66)(8)\sqrt{2/\pi}\ (\bar{\lambda}/h) = 1.15$$

Therefore, the leakage rate should be (1 + 1.15) or 2.15 times that computed from the laminar-flow equation.

If the gas is helium instead of air, we can get an approximate molecular correction factor in the following way. Kinetic theory of gases gives that the mean free path of gas molecules is proportional to viscosity and inversely proportional to the square root of molecular weight (see Eq. 6). The viscosity of helium is not too much different from that of the air while the molecular weight is about 1/7 of that of air. Therefore the molecular flow correction factor for helium is about $\sqrt{7}$ times that for air, or about 3. This shows that leakage of helium through the passage is dominated by molecular flow effect.

16

22.5 Gas Calculations

It has been shown that for a gas behaving essentially as a perfect gas leaking through an annular passage between two flanges

$$Q = \frac{wh^3(\Delta P)\bar{P}}{12\mu\ell(P/\rho)}\left[1 + \epsilon\, 8\sqrt{2/\pi}\,\frac{\bar{\lambda}}{h}\right] \tag{12}$$

where w = mean perimeter of the flange

h = clearance between flanges

ΔP = pressure difference

$\bar{P}$ = mean pressure = $\dfrac{P_{internal} + P_{external}}{2}$

μ = viscosity of the gas

ℓ = width of the flange (in the direction of leakage flow)

(P/ρ) = pressure-density ratio of the gas (a constant for a particular gas)

ϵ = molecular correction factor ($\approx .9$)

$\bar{\lambda}$ = mean free path of the gas molecules at the mean pressure, $\bar{P}$

In order to obtain a quantitative idea of leakage rate a sample channel of length $\ell = 0.1$ in. and width $w = 5$ in. (corresponding approximately to a 1.5 in. diameter tube) will be considered. Various gases (helium, hydrogen, oxygen, and nitrogen) will be used to calculate leakage at 20°C (68°F) from high pressure to atmospheric pressure for different clearances, h.

Gas properties are readily available (Refs. 1 and 10-14) although corrections are necessary to obtain values at 20°C and 1 atm. These were made using the formulae

$$\frac{\rho_1}{\rho_2} = \left(\frac{P_1}{P_2}\right) \times \left(\frac{T_2}{T_1}\right) \tag{13}$$

and

$$\frac{\lambda_1}{\lambda_2} = \left(\frac{P_2}{P_1}\right) \qquad T = const. \tag{14}$$

Property values used are tablulated below.

17

TABLE 22.1

Gas	$\rho(\#/in^3)$	λ(micro-inches)	μ(centi-poise)
He(20°C & 1 atm)	6.01×10^{-6}	10.66	.0194
H_2(20°C & 1 atm)	3.03×10^{-6}	6.78	.00931
O_2(20°C & 1 atm)	4.81×10^{-5}	3.86	.0206
N_2(20°C & 1 atm)	4.21×10^{-5}	3.61	.0184

For the case considered, w = 5 in. and ℓ = 0.1 in., T = 20°C, with an external pressure of one atmosphere,

$$Q_{He} = .4706 \times 10^{-9} h^3 (\Delta P)\bar{P} \left[1 + 61.19/h\bar{P}\right]$$

$$Q_{H_2} = .4946 \times 10^{-9} h^3 (\Delta P)\bar{P} \left[1 + 38.89/h\bar{P}\right]$$

$$Q_{O_2} = 3.549 \times 10^{-9} h^3 (\Delta P)\bar{P} \left[1 + 22.14/h\bar{P}\right] \tag{15}$$

$$Q_{N_2} = 3.478 \times 10^{-9} h^3 (\Delta P)\bar{P} \left[1 + 20.72/h\bar{P}\right]$$

where   Q = flow in lb/hr

'   h = clearance in micro-inches

ΔP and $\bar{P}$ = pressure difference and mean pressure respectively in atmospheres

Figs. 22.1 through 22.4 present the results of the calculations for laminar flow only and for the combined laminar and molecular flow as expressed by equation 12.

18

Fig. 22.1
Leakage rate for Helium at 20°C (68°F)
for an annular passage of 5 in. perimeter
and 0.1 in. length, with 1 atmosphere
external pressure.

Note: Use logarithmic interpolation

- - - - - - - Laminar flow only

———————— Corrected for molecular flow

19
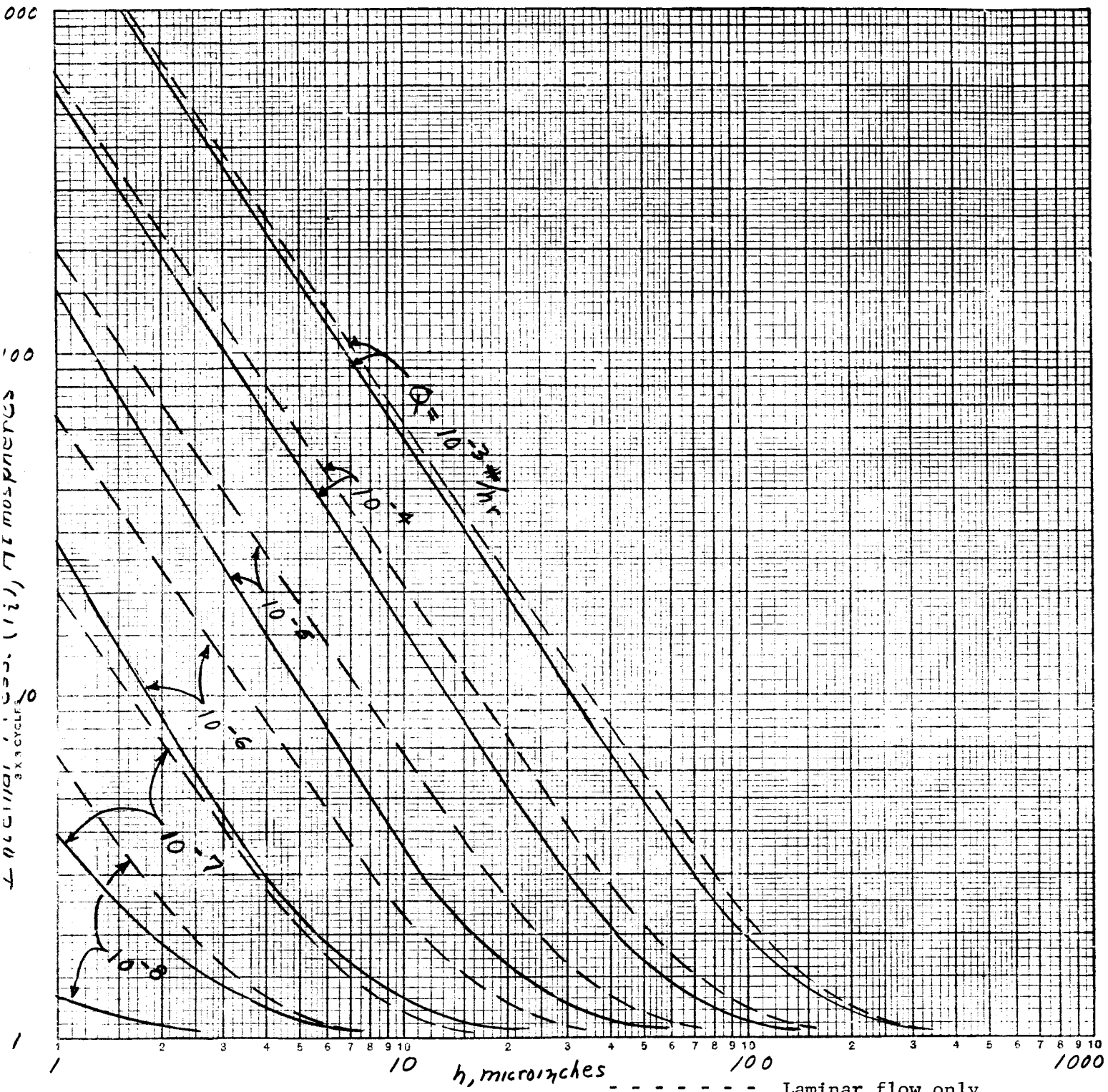
Fig. 22.2
Leakage rate for Hydrogen at 20°C (68°F)
for an annular passage of 5 in. perimeter
and 0.1 in. length, with 1 atmosphere
external pressure.

Note: Use logarithmic interpolation

- - - - - - Laminar flow only

——————— Corrected for molecular flow

20
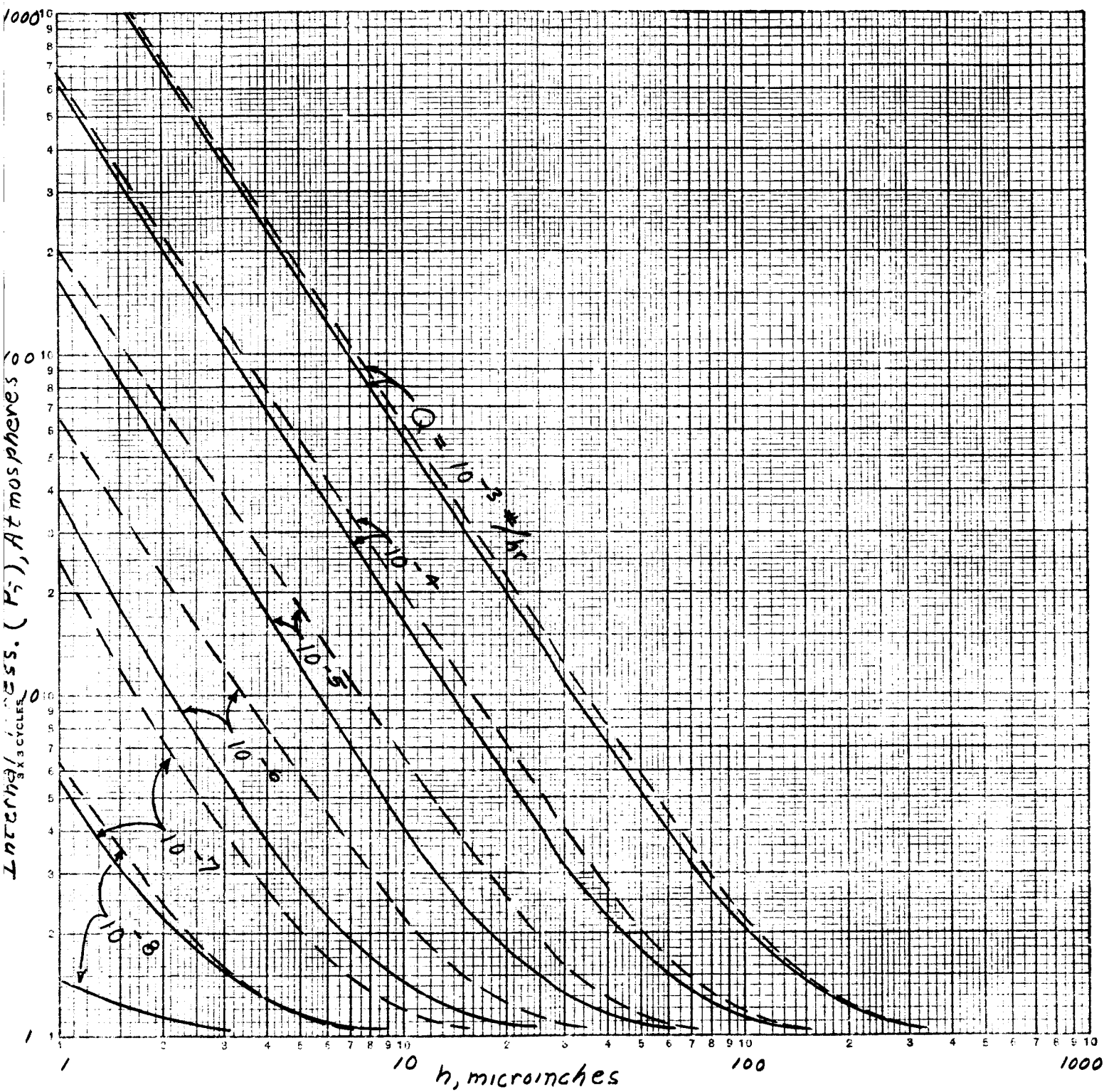
Fig. 22.3
Leakage rate for Oxygen at $20^{\circ}C$ ($68^{\circ}F$)
for an annular passage of 5 in. perimeter
and 0.1 in. length, with 1 atmosphere
external pressure.
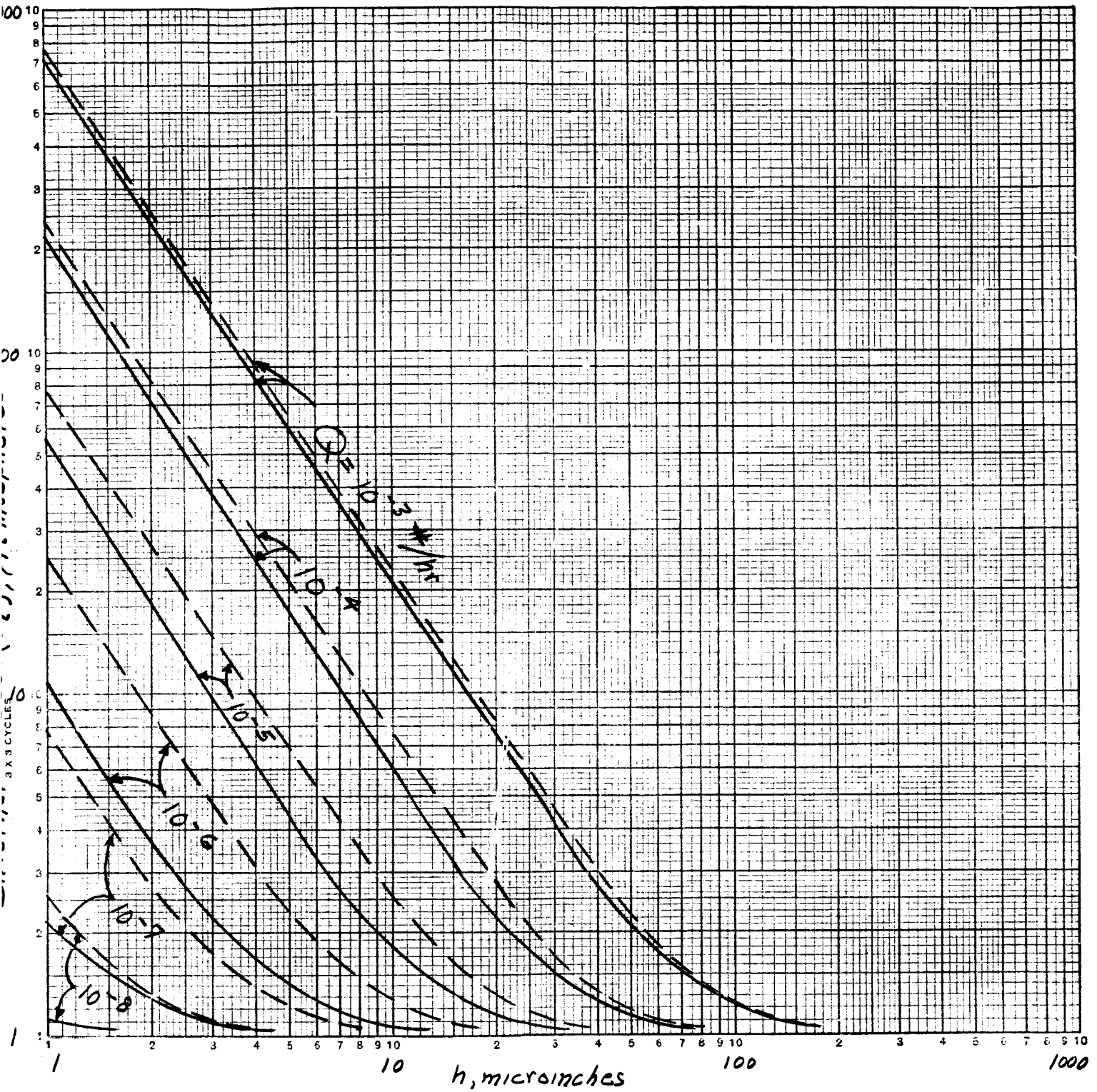
Note: Use logarithmic interpolation

------ Laminar flow only

——————— Corrected for molecular flow

Fig. 22.4
Leakage rate for Nitrogen at 20°C (68°F)
for an annular passage of 5 in. perimeter
and 0.1 in. length, with 1 atmosphere
external pressure.
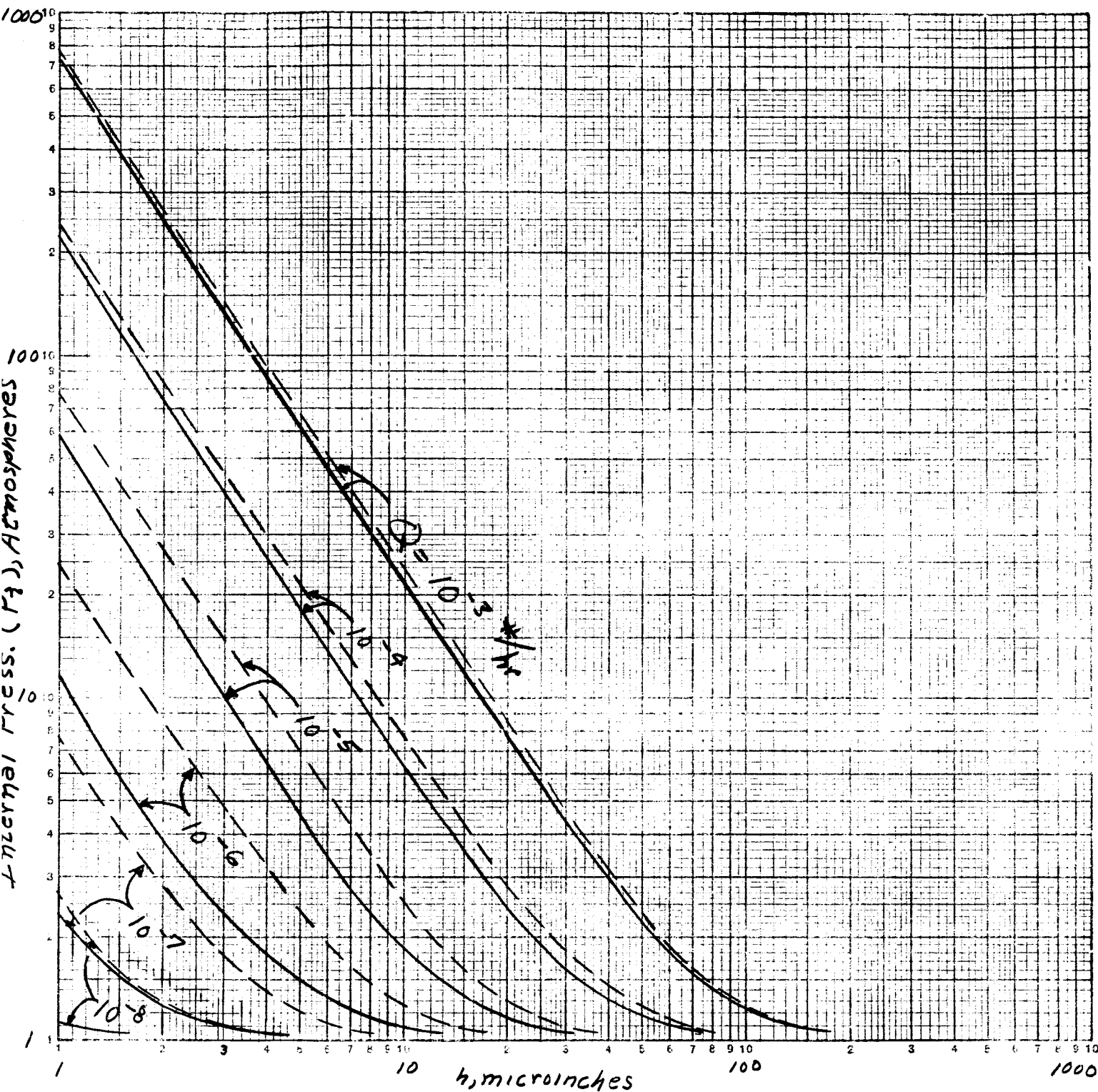
Note: Use logarithmic interpolation   - - - - - - - - Laminar flow only

——————— Corrected for molecular flow

22.6 Liquid Calculation

Equation 1 is also the basis for the calculated leakage of liquids,

$$Q = - \frac{\rho w h^3}{12\mu} \frac{dP}{dx}$$

where ρ and μ are pressure-dependent. The density relation that results from the definition of bulk modulus is

$$\rho_2 = \rho_1 \left[\frac{K}{K - (P_2 - P_1)} \right] \qquad (16)$$

where K = bulk modulus

P_1 = atm. pressure

ρ_1 = density at atm. pressure

P_2 = pressure of interest

ρ_2 = density at P_2

On the other hand, little is known concerning the pressure dependence of viscosity (Ref.15). Of the many suggested equations, the one presented by Frenkel (Ref.16) was chosen, since it does not involve emperical constants or liquid properties as yet unknown, and it has been corroborated, to some degree, by experiment. The viscosity relation is, therefore, assumed to be

$$\mu_2 = \mu_1 \exp(P_2/P_K) \qquad (17)$$

where μ_1 = viscosity at atm. pressure

P_2 = the pressure of interest

μ_2 = viscosity at P_2

P_K = that pressure which corresponds to an e(2.71...)-fold increase of viscosity

$$P_K = \frac{\alpha KT}{\gamma} \qquad (18)$$

where α = coefficient of thermal expansion
K = bulk modulus
T = absolute temperature
γ = an empirical constant ≈ 5

23

The substitution of these relationships into equation (1) results in a series solution for Q; however, an approximation can be made by first assuming ρ and μ as constants.

The result is equation 2. Now the pressure dependence is invoked by using values of ρ and μ as determined at the mean pressure. When the external pressure is one atmosphere, this yields

$$Q = \frac{\rho_1 w h^3}{12\, \mu_1 \ell} \left(\frac{K}{K - \bar{P}} \right) \frac{\Delta P}{\exp(\bar{P}/P_K)} \tag{19}$$

Calculations were carried out for liquid hydrogen, liquid oxygen and rocket fuel, RP-1, using the properties (Refs. 1, 10-14, 17) listed in Table 22.2 .

TABLE 22.2

Liquid	$\rho(\#/in^3)$	μ(centi-poise)	$\alpha\left(\dfrac{1}{°C}\right)$	K(atm)
H_2(-252.7°C & 1 atm)	.00256	.0130	13×10^{-3}	17,000
O_2(-183°C & 1 atm)	.0412	0.189	4.1×10^{-3}	15,000
RP-1(20°C & 1 atm)	.0291	1.10	$.92 \times 10^{-3}$	13,600

Again for the case of w = 5 in. and ℓ = .1 in.:

$$\left.\begin{aligned}
Q_{H_2} &= 29.9 \times 10^{-8} \left(\frac{17,000}{17,000 - \bar{P}} \right) \frac{h^3 \Delta P}{\exp(\bar{P}/880)} \\[2em]
Q_{O_2} &= 33.1 \times 10^{-8} \left(\frac{15,000}{15,000 - \bar{P}} \right) \frac{h^3 \Delta P}{\exp(\bar{P}/1100)} \\[2em]
Q_{RP-1} &= 4.02 \times 10^{-8} \left(\frac{13,600}{13,600 - \bar{P}} \right) \frac{h^3 \Delta P}{\exp(\bar{P}/850)}
\end{aligned}\right\} \tag{20}$$

where the quantities are as defined for equation 15. The results are presented as Figs. 22.5, 22.6, and 22.7.

24

Fig. 22.5
Leakage rate for liquid Hydrogen at -252.7°C
(-423°F) for an annular passage of 5 in.
perimeter and 0.1 in. length, with
1 atmosphere external pressure.

Note: Use logarithmic interpolation

25
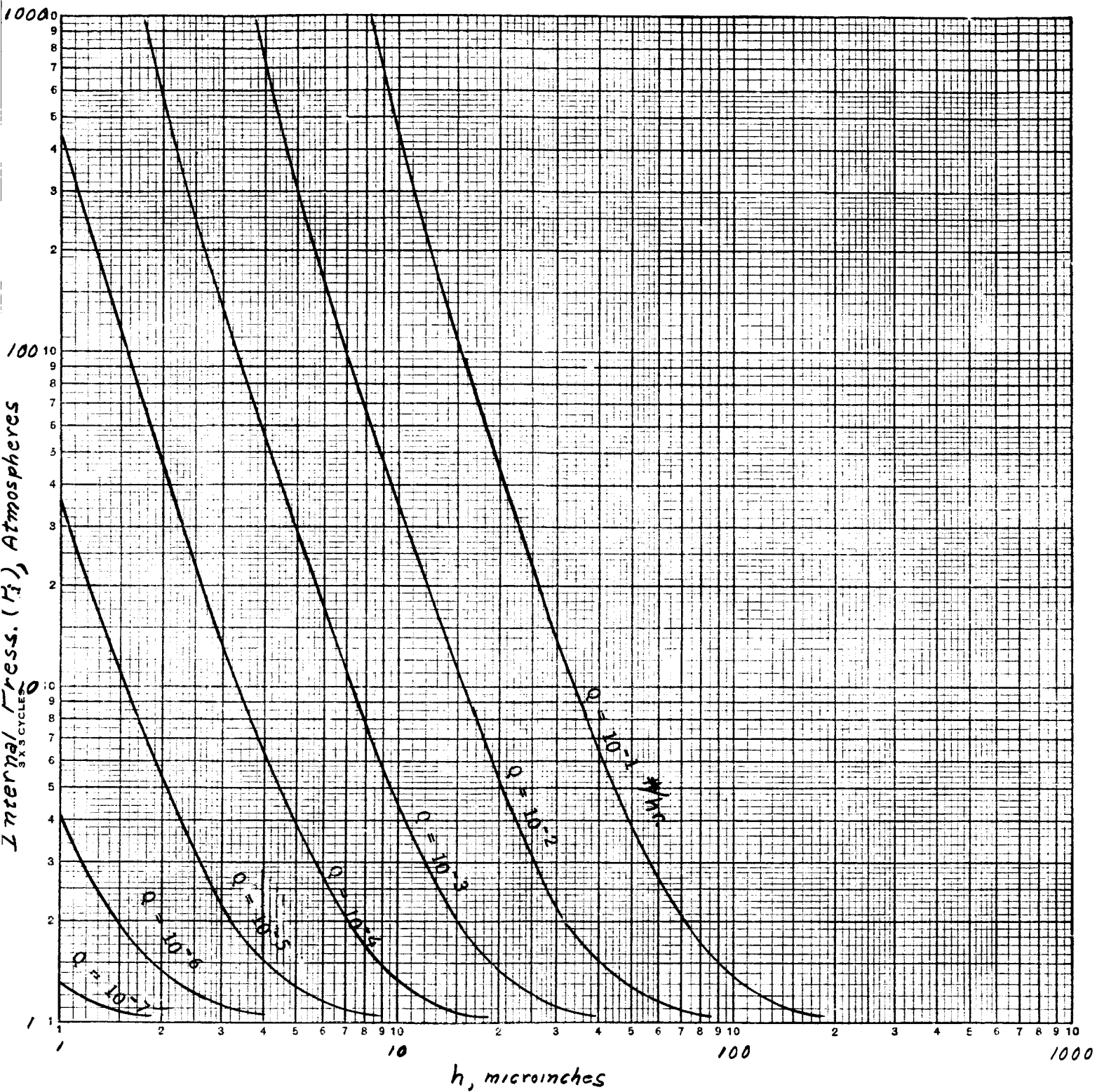
Fig. 22.6
Leakage rate for liquid Oxygen at -183°C
(-297.4°F) for an annular passage of 5 in.
perimeter and 0.1 in. length, with
1 atmosphere external pressure.

Note: Use logarithmic interpolation

26
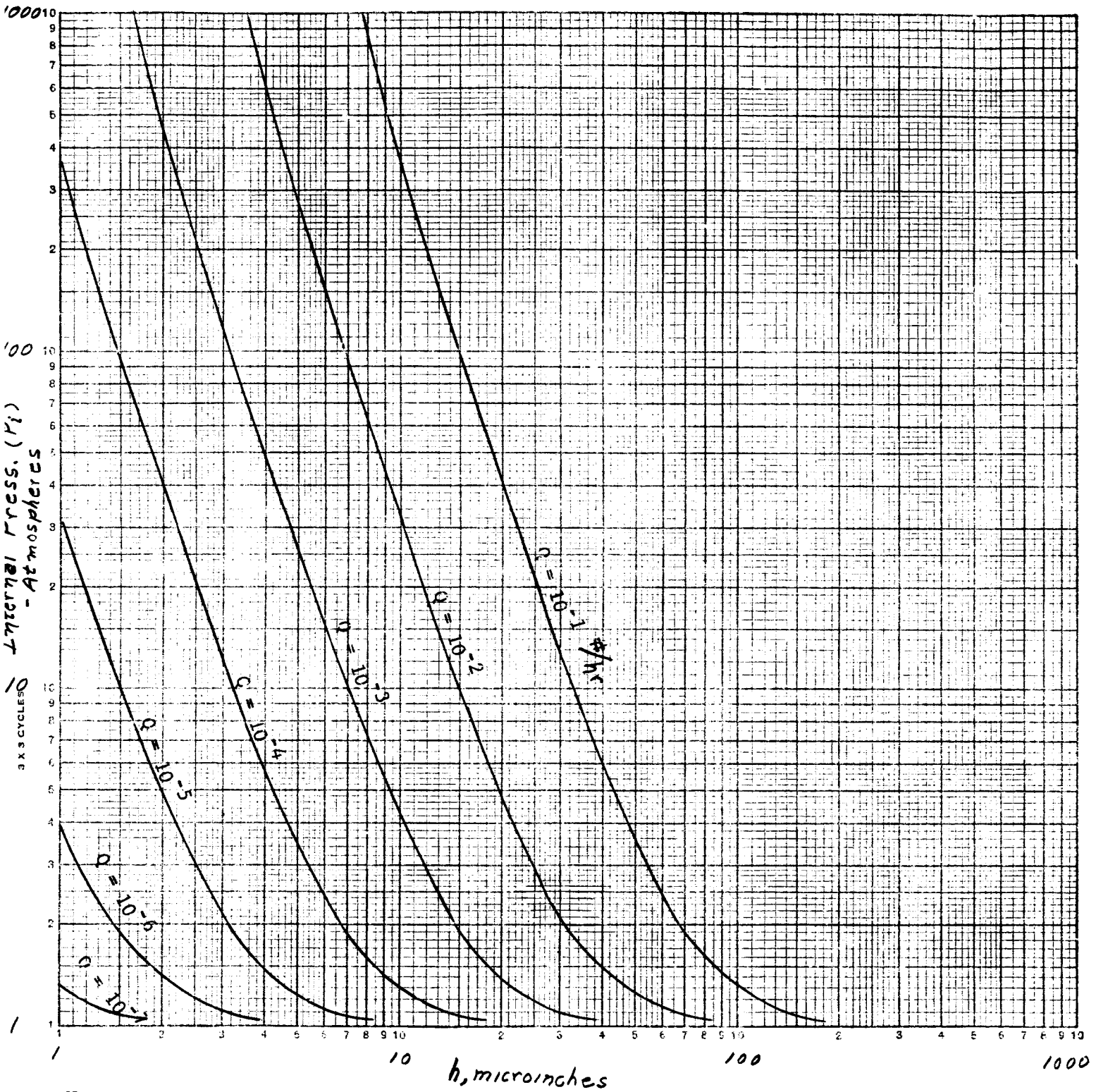
Fig. 22.7
Leakage rate for RP-1 at 20°C (68°F)
for an annular passage of 5 in. perimeter
and 0.1 in. length, with 1 atmosphere
external pressure.

Note: Use logarithmic interpolation

27
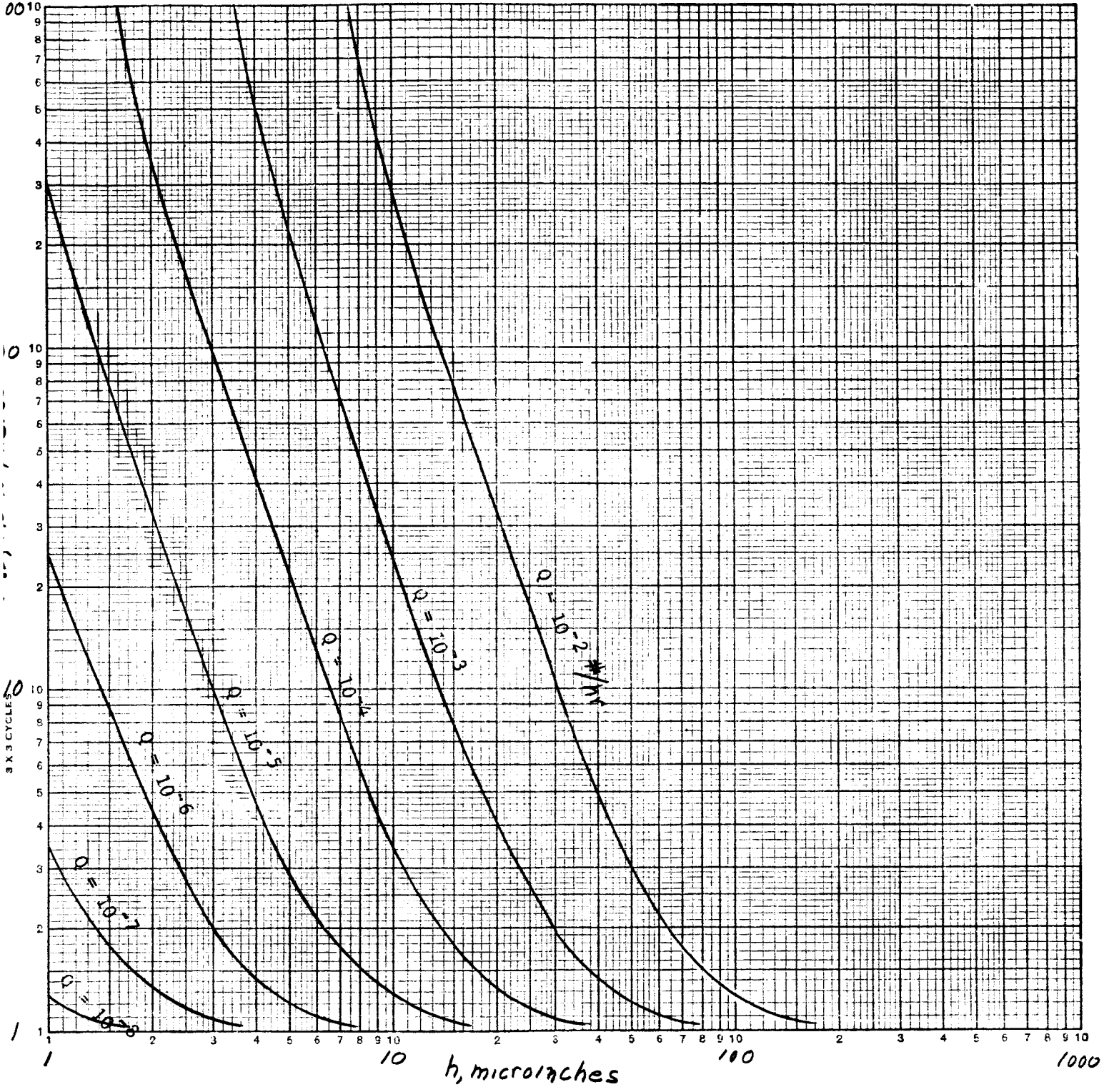
22.7 Conversion to Other Conditions

While, for the calculated leakage rates, specific dimensions and operating conditions were chosen, the resultant curves may be converted to leakage through other passages under other conditions. A convenient nomographic method of conversion can be found in Ref. 4.

(1) In all cases:

a. To convert to other passage widths, multiply the leakage rate by

$$\frac{\text{width, in.}}{5}$$

b. To convert to other passage lengths, multiply the leakage rate by

$$\frac{0.1}{\text{length, in.}}$$

(2) For gases when molecular correction is small:

a. To convert to leakage rate at other temperatures, multiply the leakage rate by

$$\left(\frac{293}{273 + \text{temperature, } ^{O}C} \right)^{x} \text{ or } \left(\frac{528}{460 + \text{temperature, } ^{O}F} \right)^{x}$$

where values of (x) for the different gases are given in Table 22.3.

b. To convert to leakage rate at other outside pressures, P_o, read the ordinate in units of

$$\frac{P_i}{P_o}$$

and multiply the leakage rate as found from the graph by

$$(P_o)^2$$

(3) For gases when molecular flow correction is not small:

a. To convert to leakage rate at other outside pressures, after applying the conversion in (1) and (2) to the given laminar flow curve, multiply the leakage rate by

$$\left[1 + C/h\bar{P} \right]$$

where values of (C) for the different gases are given in Table 22.3

(4) For liquids:

    a.   To convert to leakage rates at other temperatures, multiply the given rate by

$$\frac{\rho_2 \mu_1}{\rho_1 \mu_2} \cdot \exp\left[\frac{\bar{P}}{P_K}\left(1 - \frac{T_1}{T_2}\right)\right]$$

where ρ_1, μ_1, and T_1 are the density, viscosity and absolute temperature for which the curves are valid and which are available from Table 22.2. ρ_2, μ_2, and T_2 are the density, viscosity and absolute temperature at the temperature of interest, while the values of P_K of the liquids are given in Table 22.4

    b.   To convert to leakage rate at other outside pressures, read the ordinate in unit of

$$\frac{P_i}{P_o}$$

and multiply the leakage rate as found from the graph by

$$\frac{P_o\left[K - \frac{\bar{P}}{P_o}\right]}{\left[K - \bar{P}\right]\exp\left[\frac{\bar{P}(P_o - 1)}{P_K P_o}\right]}$$

Values of K, bulk modulus, and P_K for the different liquids will be found in Table 22.4. Due to the complexity of this conversion, in most cases it would be advisable to carry through the computation in its entirety starting with equation 11.

<div align="center">29</div>

Table 22.3

Gas	Exponent, x	Constant, C
H_e	1.653	61.19
H_2	1.678	38.89
N_2	1.702	22.14
O_2	1.721	20.72

Table 22.4

Liquid	Bulk Modulus, K(atm)	P_K(atm)
H_2	17,000	880
O_2	15,000	1,100
RP-1	13,600	850

30

22.8   Extension to Other Models

It is obvious that the channel-flow leakage model we have been consider-
ing is far from being realistic. The actual leaking passages are probably
more like many capillary tubes, of different and changing cross-sections and
intersecting each other at many places. On the one hand, the present model
can take these into consideration by properly choosing the geometrical dimen-
sions of the channel passage, based on statistical consideration of the actual
surfaces. On the other hand, the result of the present model can be extended
to such other models which describe in more detail the shapes of the actual
leaking passages. For instance, the essential difference in flowing through
tubes rather than channels is the bounding effect of the sides. In tubes, the
laminar-flow velocity profile becomes a paraboloid instead of a parabola,
resulting in smaller leakage rate for the same cross-sectional area. Many of
these flow analysis properties can be carried over from the result of the present
model by using the idea of equivalent diameter mentioned previously. A
similar situation appears in the molecular flow region.

For flow through channels of changing cross-section and interconnecting
passages, we may conceive of the flow as going through a series of very short
channels, each of constant cross-section. For flow in each short channel,
Eqs. (2) and (3) apply and we can define the impedance of the channel to the
flow as

$$\frac{\Delta P \bar{P}}{Q} = \frac{12 \mu \ell}{\rho w h^3} \quad \text{for liquids}$$

$$\frac{\Delta P \bar{P}}{Q} = \frac{12 \mu \ell R T}{m w h^3} \quad \text{for gases}$$

By properly combining these impedances (in series, in parallel, etc.) we can
obtain the picture of over-all leakage process. As an example consider the
flow of a certain liquid through a channel of gradually changing thickness.
Let us divide the channel into n short channels each of thickness d_i and
length ℓ_i. The flow impedance of each short channel is

$$12 \mu \ell_i / P \ d_i^3 = c \ell_i / d_i^3$$

From the condition that the same amount of liquid flows through all the
channels and the total pressure drop is the sum of the pressure drop across
each channel, we can easily show that the over-all impedance to flow is

$$c \sum_i^n \ell_i / d_i^3$$

Since ℓ_i / d_i^3 is inversely proportional to the cube of the thickness d_i, it
can be seen that channels of smaller thickness have greater influence in im-
peding the leakage flow.

31

22.9   Appendix

22.9.1   Entrance Length

The leakage rate equation derived in section 22.3 is based on
the assumption that in laminar flow, the velocity profile is parabolic at
each section along the passage. The actual situation is that at the immediate
entrance the boundary layer thickness is zero and the velocity profile is
uniform. The thickness increases with distance until the two layers connect
together and the velocity profile becomes parabolic. The distance from the
entrance to the point where the two boundary layers come together is called
the entrance length ℓ_e. It is apparent that in computing the leakage rate by
Eqs. (2) and (3) we should replace ℓ by $\ell - \ell_e$ and take the internal pressure
as the pressure at the end of the entrance length.

Boussinesq (Ref.5) obtained theoretically the entrance length of a
cylindrical tube as

$$\ell_e = 0.26 \, aR$$

where   a = radius

             R = Reynolds number based on the radius

For a channel passage the entrance length will be somewhat longer. A good
estimate can be made from our knowledge of the growth of boundary layer
thickness δ for a flat plate (Ref.6).

$$\delta \sim \sqrt{\mu x / \rho v}$$

where   x = distance from the entrance.

When the boundary layers come together, the boundary layer thickness = h/2.
From the above relations we have

$$h/2 \quad \sqrt{\mu \ell_e / \rho v}$$

or $\ell_e \sim Rh/4$

For leakage rates of interest to us, the leakage velocity is small and the
clearance h very small so that the entrance length is also very short. It
is generally permissible to neglect this entrance length in computing the
leakage rate.

We have stated that the correct internal pressure to be used in computing
leakage rate is that at the end of entrance length. As long as the entrance
length is very short and the leakage rate is small, the difference between the
pressures at the entrance and at the end of entrance length is negligible.

22.9.2 Consideration of Inertia and Temperature Variation

Most of the leakage rates of interest to us belong to the group treated previously. For compressible gases at large leakage rates the effect of inertia and temperature variation may become of importance. We shall treat these effects in this section and illustrate that with a large pressure difference the leakage speed as well as the leakage rate can become considerable even for small clearances.

When inertia is taken into consideration, the equation of motion of the fluid becomes

$$\rho v \frac{dv}{dx} = - \frac{dP}{dx} - \frac{12\mu}{h^2} v \tag{21}$$

which says that the change in momentum is equal to the difference between pressure gradient and the viscous friction at the walls. The last term is obtained by assuming that the velocity gradient at the wall is the same as the incompressible parabolic velocity profile. Dividing the equation by ρv^2 and integrating, we obtain

$$\ln \frac{v_1}{v_2} = - \frac{1}{\rho v} \int_2^1 \frac{dP}{v} - \frac{12\mu}{\rho v d^2} (x_1 - x_2) \tag{22}$$

where 1 and 2 are two sections along the channel. By making use of the constant mass flow condition

$$Q = \rho v w h = constant \tag{22a}$$

we can express the integral $\int_2^1 dP/v$ as $(1/\rho v) \int_2^1 \rho dP$.

Still we cannot evaluate this integral until we know the relation between the density and pressure along the channel from section 1 to section 2. This relation depends on the heat transfer between the gas and the channel walls. We shall consider two extreme cases:

    (1)   Infinite heat transfer so that the leakage is under isothermal conditions.

    (2)   No heat transfer at all.

Actual cases lie in between these two extremes. In case (1) we have the additional isothermal condition.

33

$$P/\rho = RT/m = constant$$

and in case (2) we have the conservation of energy relation

$$c_p T + v^2/2 = \text{constant}$$

where c_p = specific heat under constant pressure.

With these relations we are able to integrate Eq. (22). The results are, for case (1)

$$\ln \frac{M_1}{M_2} + \frac{1}{2\gamma} \left(\frac{1}{M_1^2} - \frac{1}{M_2^2} \right) = \frac{12\mu}{\left(\frac{Q}{wh}\right) h^2} (x_2 - x_1) \tag{23}$$

and for case (2)

$$\frac{\gamma+1}{2\gamma} \ln \frac{M_1 \sqrt{1 + \frac{\gamma-1}{2} M_2^2}}{M_2 \sqrt{1 + \frac{\gamma-1}{2} M_1^2}} + \frac{1}{2\gamma}\left(\frac{1}{M_1^2} - \frac{1}{M_2^2} \right) = \frac{12\mu}{\left(\frac{Q}{wh}\right) h^2} (x_2-x_1) \tag{24}$$

where M = Mach number

         γ = ratio of specific heats at constant pressure and at constant volume.

These equations involve two unknowns which are Mach numbers at sections 1 and 2. An additional equation which gives the relation between M_1 and M_2 is

$$\frac{M_2}{M_1} = \frac{P_1}{P_2} \quad \text{for case (1)} \tag{25}$$

and

$$\frac{M_2 \sqrt{1 + \frac{\gamma-1}{2} M_2^2}}{M_1 \sqrt{1 + \frac{\gamma-1}{2} M_1^2}} = \frac{P_1}{P_2} \quad \text{for case (2)} \tag{26}$$

The leakage rate Q is given by the following formula

$$Q = (wh) \left(M_1 P_1 \sqrt{\gamma m/RT_1} \right)$$
$$= (wh) \left(M_2 P_2 \sqrt{\gamma m/RT_2} \right) \tag{27}$$

We can compute the leakage rate from the above equations by taking section 1 and 2 as entrance and exit of the channel.

An important consequence of taking inertia into consideration is that it can be shown from Eq. (23) and (24) that the flow in the channel can never become supersonic, whatever the pressure difference may be. The same conclusion is true for the flow of liquids.

31

22-26

Generally speaking the Mach number at entrance is much smaller than the Mach number at exit. Under this condition both Eq. (23) and (24) simplify to

$$\frac{1}{2\gamma}\left(\frac{1}{M_1^2}\right) = 12\mu \ (x_2 - x_1)/\left(\frac{Q}{wh}\right) h^2 \tag{28}$$

Substituting in Eq. (27) we obtain the leakage rate as

$$Q = \frac{mwh^3 p_1^2}{24\mu \ (x_2 - x_1)RT} \tag{29}$$

which is in agreement with Eq. (3) of section 2.3 when the internal pressure is large. This extends the validity of Eq. (3) derived previously to the present case when the temperature and inertia effect are considered.

We shall illustrate the results with the following numerical example:

    Geometry of leakage channel

      length = 0.1 in.

      width =   5 in.

      clearance = 50 x 10^{-6} in.

Air at 60°F is leaking out from a pressure of 100, 50, 20, 10, 5, 2 atm. to atmospheric pressure.

    Properties of air at 60°F are

      density = 1.15 x 10^{-7} lb-sec^2/in^4 at atmospheric pressure

      viscosity = 2.62 x 10^{-9} lb-sec/in^2

      Ratio of specific heats $\gamma = 1.4$

The numerical result is summarized in the following table:

<p align="center">35</p>

| Entrance | | Exit | | Leakage Rate |
Pressure Atm.	Mach No.	Pressure atm.	Mach No.	lb/hr
100	0.0438	3.98 (adiabatic)	1	2.33
50	0.0219	1.99 (adiabatic)	1	5.83×10^{-1}
20	0.00876	1	0.175	9.36×10^{-2}
10	0.00438	1	0.0438	2.37×10^{-2}
5	0.00210	1	0.0105	5.58×10^{-3}
2	0.00656	1	0.00131	6.98×10^{-4}

These examples show that

(1) For large pressure difference both the leakage speed at exit and the leakage rate are considerable. For instance, more than two pounds of air will leak out in an hour if the internal pressure is 100 atm. (1470 psi)

(2) Even at the leakage rate of 2.33 lb/hr, the corresponding Reynolds number can be computed as only 128. Turbulent flow does not occur.

36

22.10 References

1. S. Dushman and J. M. Lafferty, Scientific Foundations of Vacuum Technique, Second Ed., Wiley, 1962.

2. E. H. Kennard, Kinetic Theory of Gases with an Introduction to Statistical Mechanics, McGraw-Hill, 1938.

3. A. E. Scheidegger, The Physics of Flow Through Porous Media, Macmillan, 1957.

4. D. J. Santeler and T. W. Moller, Leak Detection I - Fluid Flow Conversion in Leaks and Capillaries, General Electric Company TIS Report 56GL261, 1956.

5. L. Prandtl and O. G. Tietjens, Applied Hydro- and Aeromechanics, Dover, 1957.

6. H. W. Liepmann, and A. Roshko, Elements of Gas Dynamics, Wiley, 1957.

7. L. Howarth, Modern Developments in Fluid Dynamics, High Speed Flow, Vol. 1, Oxford, 1953.

8. H. Schlichting, Boundary Layer Theory, McGraw-Hill, 1955.

9. H. Rouse, Elementary Mechanics of Fluids, Wiley, 1946.

10. Handbook of Chemistry and Physics, 41st Edition, 1959.

11. Handbook of Chemistry, 10th Edition, 1961.

12. Smithsonian Physical Tables, 9th Edition, 1951.

13. O. W. Eshbach, Handbook of Engineering Fundamentals, Wiley, 1936.

14. International Critical Tables, 1930.

15. Second Report on Viscosity and Plasticity, North Holland Pub. Co., 1938.

16. J. Frenkel, Kinetic Theory of Liquids, Dover, 1955.

17. RP-1 data via telephone conversation with John Halliday, Malta Test Station, from a brochure by Aerojet.

23. GAS PERMEATION THROUGH SOLIDS*

by

H. J. Sneck

23.0 Summary

The gases used in rocket propulsion systems can permeate solid walls
of metals or polymers by a molecular diffusion process. The rate of per-
meation flow is very slow compared to leak rates encountered in conventional
engineering practice and is well below zero leakage as determined by a
bubble test (Section 21). However, permeation flow can be readily measured
by a mass-spectrometer leak detector. To achieve the ultimate in leak-
tightness, especially in long space voyages, and to make accurate measure-
ments of leakage, the possibility of flow through solid pipe walls and
solid gaskets must be considered.

This section presents a compilation of permeation flow data obtained
by Dr. F. J. Norton of the General Electric Research Laboratory and others
who have worked in this field. The order of magnitude of the permeation
effect is illustrated by numerical examples at the end of this Section.

37

23.1 The Permeation Process

The process whereby gases pass through sound solid membranes is described by Norton (Ref. 1) as follows:

1. The gas on the high-pressure side is first adsorbed and dissolved in an external surface layer on the membrane surface. Surface pre-treatment is important here.
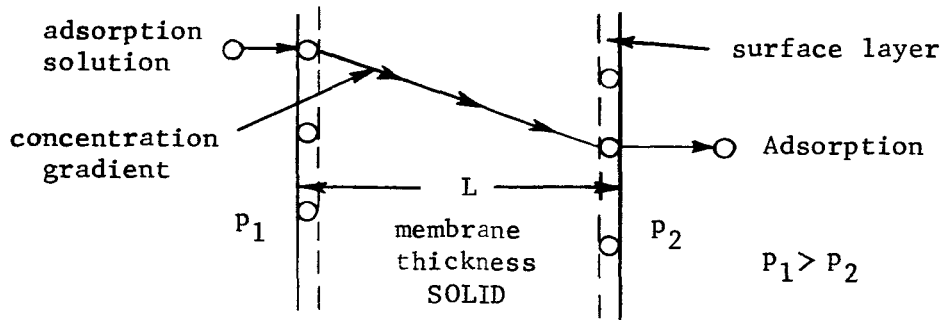
FIGURE 23.1 Permeation of Gas Through a Solid Membrane

2. The gas then diffuses through the "solid" driven by the concentration gradient according to Fick's Law. The diffusion of the gas may be as atoms of a dissociated molecule if the membrane is metallic, or molecules if the membrane is a polymer.

3. When the gas reaches the low-pressure side of the membrane, it undergoes a transition from a dissolved state to an absorbed state and is desorbed at the surface and passes into the surroundings (where it will reassociate if the diffusion was atomic). Again surface pretreatment may be important.

The overall steady-state process described above is termed "permeation", and the speed of the permeation process is controlled by the slowest of the above steps.

There are very few generalities one can make for the permeation process as a whole. Norton (Ref. 2) gives the known generalities as follows:

Gas Permeation Through

Metals	Polymers
No rare gas passes through any metal (and Halogen gases to no marked degree - Ref. 11)	All gases permeate all polymers
H_2 permeates most metals, especially Fe	H_2O rate apt to be high
O_2 permeates Ag	
H_2 through Fe by corrosion, electrolysis	Many specificities
Permeation rates vary as $\sqrt{\text{pressure}}$	Permeation rates vary as pressure

where S = solubility.

$$-\frac{\partial c}{\partial x} = -S\frac{\partial p}{\partial x} = S\frac{\Delta p}{L}$$

Under this condition the diffusion coefficient is, in general, constant so that equation 2 may be written for a membrane of uniform thickness as

$$Q = DSA\frac{\Delta p}{L} \tag{4}$$

where Δp = pressure drop across the membrane.
    If the permeation rate is defined as

$$P = DS \tag{5}$$

equation 4 becomes equation 1.

    It should be noted that equation 1 is strictly applicable only if the diffusion is molecular in nature, as in polymers. Some exceptions to Henry's Law have, however, been noted for rubber by Jost (Ref. 3). If the diffusion process is atomic in nature, as with diatomic gases permeating through metals, Equation 1 is not strictly applicable. Dushman (Ref. 4) indicates that when the diffusion is atomic

$$Q \propto (\sqrt{P_1} - \sqrt{P_2}) \tag{6}$$

The permeation rate (P) used in Equation 1 is exponentially temperature dependent according to Equation 7, as illustrated in Figure 23.2 (Ref. 5).
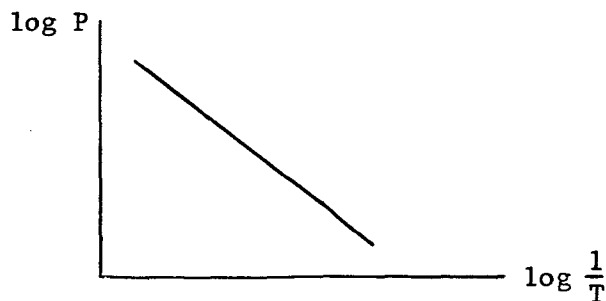
FIGURE 23.2   Exponential Temperature Dependence
of Permeation Rate

$$P = P_o \exp\left(-\frac{E}{jrT}\right) \tag{7}$$

where

P_o = constant, independent of temperature variation

E = activation energy of permeation

j = dissociation number (2 for diatomic gases permeating metals)

R = 1.986 cal/K°

T = degrees Kelvin

This equation is particularly useful in extrapolating permeation rates to higher or lower temperatures.

23.3 Permeation Rates and their Application to Calculations

The calculation of leakage rates due to permeation hinges on the experimental determination of the permeation rates (P) as defined by Equation 1. For polymers, experimental permeation rates can be extrapolated to different temperatures using Equation 7 and then applied directly in Equation 1.

The problem is not quite so straight-forward for metals where Equation 6 applies rather than Equation 1. One finds that the literature contains permeation rates for metals as defined by Equation 1. These rates are still exponentially temperature dependent as given by Equation 7, but they are correct only for the specific pressure difference given in their units (e.g., 1 torr or 1 mm Hg, 1 cm of Hg, 1 atmosphere). If the experimental values were determined when p_2 was very nearly equal to zero, and the case to be calculated also has p_2 very nearly equal to zero, then pressure extrapolations can be made using the simplified proportion.

$$\frac{Q_{actual}}{Q_{experimental}} = \sqrt{\frac{P_{1 \ actual}}{P_{1 \ experimental}}} \qquad (8)$$

Otherwise extrapolations must be made according to Equation 6. Equation 8 is particularly useful when comparing, roughly, the results of different experimenters (Ref. 4).

Considerable care must be exercised when collecting permeation rate data from the literature for the following reasons:

23.2 Permeation Equations

The volumetric flow rate (S.T.P.) for the molecular permeation of a gas through a "solid" is described by the equation

$$Q = PA \frac{\Delta p}{L} \qquad (1)$$

where

Q = volumetric flow rate at STP

A = area normal to the flow

Δp = pressure drop along the flow path

L = Length of the flow path

P = permeation rate

This equation can be derived from Fick's Law of diffusion

$$Q = -DA \frac{\partial c}{\partial x} \qquad (2)$$

where

D = diffusion coefficient $\dfrac{cm^2}{sec}$

$\dfrac{\partial c}{\partial x}$ = concentration gradient

if the solubility is small. The concentration for very small solubility is related to the pressure through Henry's Law

$$c = Sp \qquad (3)$$

39

1) Some of it is in error (as pointed out by Dayton, Ref. 5) - particularly that given by Jost (Ref. 3) and Barrer (Ref. 6).

2) The temperature must be noted because of the exponential dependence.

3) At least four different sets of units have been used for the permeation rates. They are

a) $$\frac{cm^3 - mm}{sec - cm^2 - torr}$$

b) $$\frac{cm^3 - cm}{sec - cm^2 - atm}$$

c) $$\frac{cm^3 - mm}{sec - cm^2 - atm}$$

d) $$\frac{cm^3 - mm}{sec - cm^2 - cm \, Hg}$$

This complicates the comparison of permeation rates of gases through metals for the reasons given above.

4) There are many specificities with regard to the membrane material (especially polymers) or pretreatment of materials (metals). This complicates the comparison of permeations for the same apparent material-gas combination.

Table 23.1 represents the consensus of data gathered from the references already cited as well as References 7 and 8. (It is worth noting here that when searching German-language literature the key word, permeation, is translated as "Gasdurchlässigkeit"). All data are for approximately $25^{\circ}C$ ($68^{\circ}F$).

42

TABLE 23.1 Permeation Rates (cm^3-mm/sec-cm^2-atm)
at Room Temperature

	Hydrogen	Oxygen	Nitrogen	Helium
Iron	4 to 15 x 10^{-9}		4.2 x 10^{-19}	
Steel (low carbon)	3 x 10^{-10}			
Steel (27% chrome)	1 x 10^{-12}			
Aluminum	3.1 x 10^{-22}			
Natural rubber	1.5 to 4.0 x 10^{-6}	1.8 x 10^{-6}	1.0 x 10^{-6}	3.0 x 10^{-6}
Neoprene	1.0 x 10^{-7}	0.3 x 10^{-7}	0.1 x 10^{-7}	0.6 x 10^{-7}

The following permeation-rate data for air were obtained from References 9 and 10.

Permeation rate P in $\dfrac{cm^3\text{-mm}}{sec\text{-}cm^2\text{-atm}}$ at Temperature

	$75^{\circ}F$	$176^{\circ}F$	$350^{\circ}F$
Butyl Rubber	0.02 x 10^{-6}	0.32 x 10^{-6}	6.1 x 10^{-6}
Silicone Rubber	22.0 x 10^{-6}	45 x 10^{-6}	112 x 10^{-6}
Kel-F	—	0.8 x 10^{-6}	—

While the data above appear skimpy, they represent the result of gleaning many different sources and careful comparison of the data for consistency.

The only gases cited in the literature surveyed were H_2, O_2, N_2, Xe, Ar, He and Air. None of the exotic gases or vapors, particularly fluorine compounds, were encountered in the references. Cupp (Ref. 11) indicates that the halogen gases do not permeate metals to any marked degree; and if this is true, then they might be lumped in with the rare-gas generalization.

The only metals encountered were Fe (composition of alloying elements sometimes specified), Cu, Ni, Ag, Au, Al. Here wide variations in permeability are encountered, due to differences in composition, surface condition, heat treatment, etc. Private conversations with F.J. Norton at the General Electric Research Laboratory brought out the fact that hydrogen permeates metals at the highest rate of any of the gases. Hydrogen data can therefore be used to predict the upper limit of leakage loss for any metal in question.

43

A considerable amount of data is available for polymers. Some of the more common types have been chosen to indicate the order of magnitude of permeation rate and to indicate that the losses can be great if the polymers are not chosen properly (see Numerical Example). In a current article by Frank (Ref. 12), he indicates that recent work on polymers has taken two directions:

1. Development of new polymers of low permeability (Mylar, Saran (Ref. 1), polyvinyl alcohol).

2. Treatment of polymers already available to decrease their permeability (impregnation with fillers, metal-coating the surface).

44

23.4 Numerical Example

In order to get a "feel" for the flow losses attributable to permeation, consider the following example:

A gasket 0.1" thick, 0.1" wide, and 5" nominal diameter with a 1 atmosphere pressure difference across it.
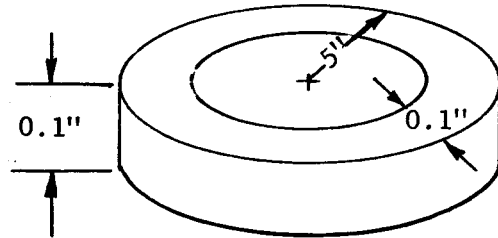
Fig. 3

$$A = 5(2.54) \, \pi \, (0.1)(2.54) = 10.13 \text{ cm}^2$$

$$L = 0.254 \text{ cm} = 2.54 \text{ mm}$$

$$\Delta p = 1 \text{ atm.}$$

Equation 1 becomes

$$Q = PA \frac{\Delta p}{L} = \frac{10.13}{2.54} \, P = 3.99 \, P$$

For a natural rubber gasket at 25°C

	P $\dfrac{\text{cm}^3 - \text{mm}}{\text{sec} - \text{cm}^2 - \text{atm}}$	Q $\dfrac{\text{atm cc}}{\text{sec}}$	ρ $\dfrac{\text{lb.}}{\text{cm}^3}$	Loss $\dfrac{\text{lb.}}{\text{year}}$
H_2	4.0×10^{-6}	15.96×10^{-6}	1.83×10^{-7}	92.0×10^{-6}
O_2	1.8×10^{-6}	7.18×10^{-6}	29.2×10^{-7}	661.0×10^{-6}
N_2	1.0×10^{-6}	3.99×10^{-6}	25.5×10^{-7}	321.0×10^{-6}
He	3.0×10^{-6}	11.97×10^{-6}	3.65×10^{-7}	137.7×10^{-6}

45

For a Neoprene gasket at $25^{\circ}C$

	P $\dfrac{cm^3 - mm}{sec - cm^2 - atm}$	Q $\dfrac{atm\ cc}{sec}$	ρ $\dfrac{lb.}{cm^3}$	Loss $\dfrac{lb.}{year}$
H_2	10×10^{-6}	3.99×10^{-6}	1.83×10^{-7}	2.30×10^{-6}
O_2	0.3×10^{-6}	1.2×10^{-6}	29.2×10^{-7}	110.0×10^{-6}
N_2	0.1×10^{-6}	0.399×10^{-6}	3.65×10^{-7}	32.1×10^{-6}
He	0.6×10^{-6}	2.4×10^{-6}	3.65×10^{-7}	27.6×10^{-6}

By way of comparison, a 10-foot-long steel pipe of the same diameter and thickness would lose Hydrogen at a rate comparable to those given above.

In conventional engineering practice, gas losses of the order shown above would, of course, be of no practical concern. When these figures are multiplied by perhaps 100, to allow for the presence of many such sealing devices in a space-craft, however, the order of magnitude begins to have significance. This is particularly true of vehicles for very long missions, where launch weight will be critical and a minimum amount of fuel will be carried.

46

23.5 References

1. F. J. Norton, "Permeation of Gases Through Solids," *J. of Applied Physics*, Vol. 28, p. 28-34 (1957)

2. F. J. Norton, "Gas Permeation through the Vacuum Envelope," General Electric Research Labratory Report No. 61-RL-2874C, Nov. 1961

3. W. Jost, *Diffusion*, Academic Press, 1951.

4. S. Dushman and J. M. Lafferty, *Scientific Foundations of Vacuum Technique*, Second Edition, Wiley, 1962.

5. B. B. Dayton, "Relations Between Size of a Vacuum Chamber, Outgassing Rate, and Required Pumping Speed," *Vacuum Symposium Transactions*, 1959.

6. R. M. Barrer *Diffusion in and through Solids*, Macmillan, 1941.

7. W. Espe, *Werkstoffkunde der Hochvakuumtechnik*, Deutscher Verlag der Wissenschaften, 1959.

8. M. von Ardenne, *Tabellen der Elektronphysik. Ionenphysik und Übermikroscopie*, Band II, Deutscher Verlag der Wissenschaften.

9. Hayes, Smith, Kitchen, "Development of High Temperature Resistant Rubber Componds," WADC Technical Report 56-331, February 1958.

10. J. S. Islinger, "Research and Development of Design Concepts for Sealing Applications in Aerospace Vehicle Cabins," Armour Research Foundation ASD Technical Report 61-696, February 1962.

11. C. R. Cupp, "Gases in Metals," *Progress in Metal Physics*, Vol. 4, Pergamon Press, 1953.

12. R. C. Frank, "Gases in Solids," *International Science and Technology*, No. 9, Sept. 1962.

47

24. WELDED, BRAZED, AND SOLDERED JOINTS

by

G. W. Hume

24.0 Summary

Permanent joints between metal pipes and tubes can be made by the conventional joining techniques such as welding, soldering, brazing, and swaging (cold welding). When properly designed and fabricated, such joints can have the same leak tightness as the base metal itself. Welded, soldered, and brazed joints can be designed for a limited number of disassemblies and reassemblies, but their main application is for permanent joints such as the pipe-to-flange joints in a flange connector.

This brief discussion of metal joining techniques is included to give a comparison between these types of joints and gasketed joints, and to provide design information on the permanent joints (such as pipe-to-flange joints) used in separable fluid connectors.

48

24.1 Introduction

Extensive research and development of true hermetic seals has been made on other programs; however, permeation of the joints by gases and liquids over long periods of time and temperature cycling has not been evaluated, although the permeation through the joints should be in the same order of magnitude as that of the metal members. Liquid or gas permeation through solid metals is a function of time and temperature as well as the chemical makeup of the system (Sec. 23). Hydrogen and oxygen are the two gases most likely to create a permeation problem, as hydrogen permeates most metals if high-temperature cycling conditions are of long duration. Permeability of gases (Ref. 1) generally increases with plastic deformation; therefore stresses should be minimized. Each application will require a specific gas permeation study once the materials and processes for the application are established. The variables are many in these applications and because of this, the author will generalize in order to give the designer a broad look at the problem of fabricating metal joints.

In the welding field a joint is considered vacuum tight if it can pass the mass spectrometer leak test. In critical applications a pressure of 50 psi of helium is placed on one side of the joint and a vacuum on the other and allowed to stand for four hours under this condition. A reading is then taken on the mass spectrometer which will detect leaks of helium in the order of 1×10^{-10} atm. cc/sec. A joint is considered leak tight if it passes this test (i.e., if no leakage is detected by the mass spectrometer) and passes non-destructive tests such as x-rays, ultrasonic, and dye penetration. The applications to be considered here would require the extension of the above test to include the thermal cycling of the system through the temperature range needed for the application and testing it during the operation. In studying the different methods of making such junctions to stainless steel and aluminum, the following factors are considered prime requirements of an ideal hermetic seal:

1. Reliability
2. Ease of non-destructive leak testing
3. High strength
4. Ease of repair
5. Fabricated with minimum effort
6. Equally easy to fabricate in field
7. Ability to withstand extremes of temperature, vibration, and shock

The temperature range of $-420^{\circ}F$ to $+2500^{\circ}F$ encountered in launch vehicles is restrictive for these applications in that a number of joining processes are likely to be needed to cover every application.

Thermal expansion of the metals in the system is another important consideration when the temperature limits are as wide as in these applications. Ideally all members should expand at the same rate over the entire temperature range in order to avoid building up internal stresses which subsequently result in cracks in the system.

24.2 Welding

Welding is not normally considered for use in an application requiring many separations during its life; however, with proper design it has been accomplished. There are a number of fusion welding processes available; however, the applications of tubing and pipes lead one to consider the non-consumable inert arc welding process as the chief source of heat.

In the case of inert arc welded seals (Ref.2), typical designs are shown in Fig.24.1 which can be machined or sawed apart. No oil or grease should be used during cutting since these materials are detrimental to the reweld operation. Since no heat is used to reopen the weld, the two mating faces can be rewelded a number of times depending on the length of the lip preparations.

The inert arc welding process eliminates the expansion problem to a large degree as no foreign metal need be added to the metals in question. Differences in expansion can arise, depending on the rate of heating or cooling thin and thick sections of the system.

50

CUT OFF

INERT ARC WELD   AFTER WELDING   REWELD

INERT ARC WELD

CUT OFF   REWELD

BEFORE WELDING   AFTER WELDING

INERT
ARC WELD

CUT OFF   REWELD

BEFORE WELDING   AFTER WELDING
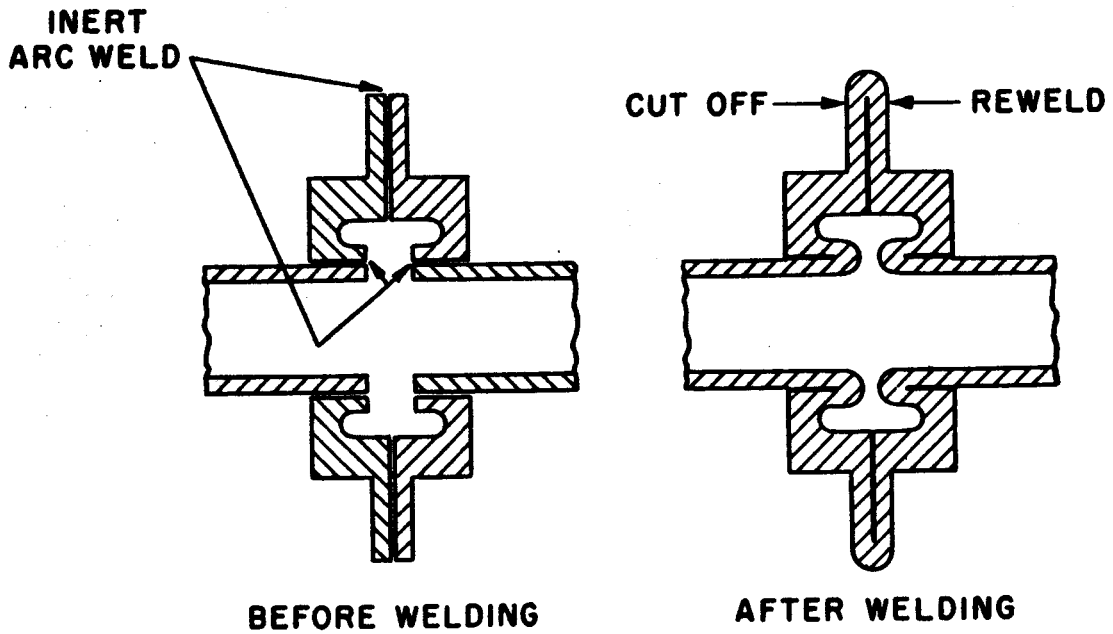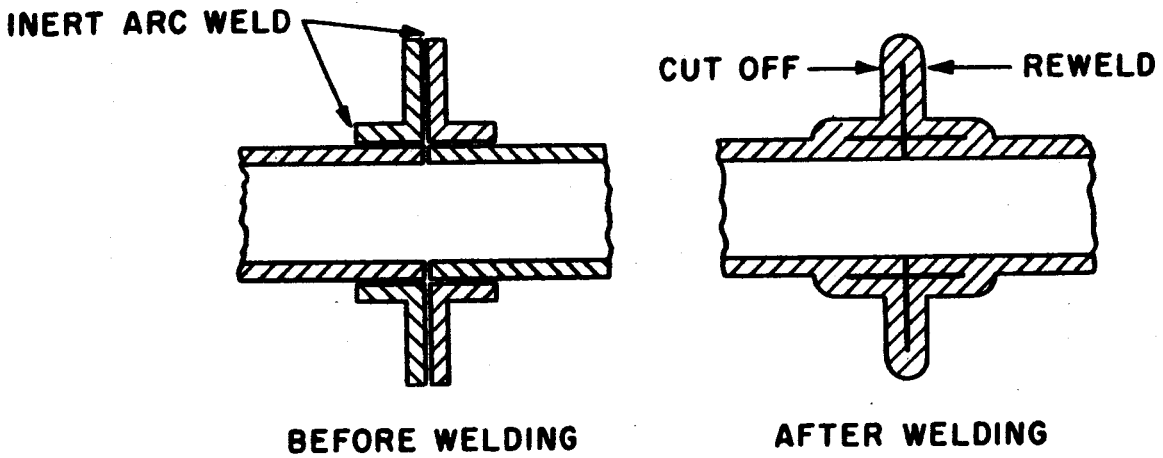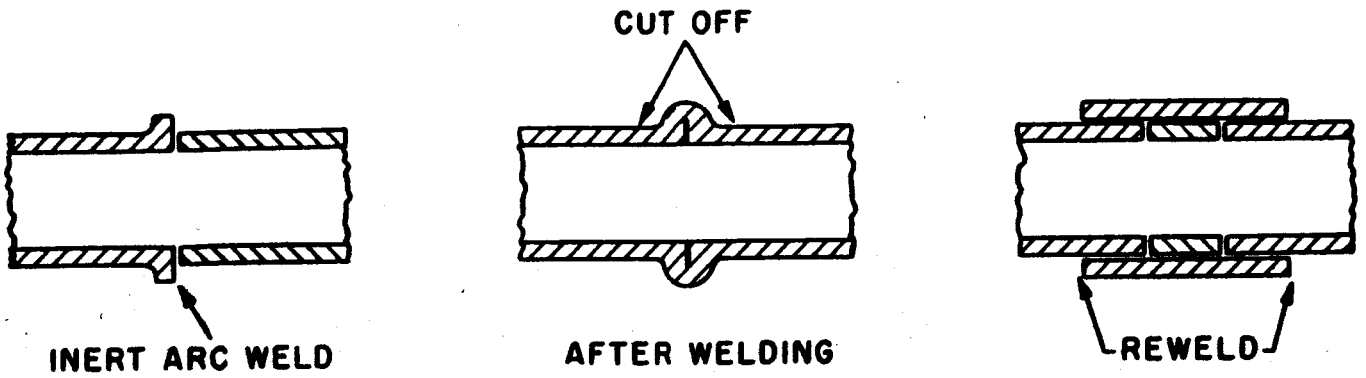
FIG. 24.1 Typical Designs of Inert Arc Welded Seals

24.3 Brazing and Soldering

It is apparent that brazing, soldering, and the base metal aluminum could not be used for sealing in the higher temperature range applications because of their low melting points and poor strength at elevated temperatures.

Brazed and soldered filler metals inherently have large differences in expansion from the base metals; however, in the lower temperature ranges they exhibit good ductility which overcomes the stress problem. Oxygen permeates silver easily; therefore in selecting braze alloys containing silver, one must use discretion as to the time and temperatures involved with oxygen in the system.

Reusable seals are difficult to design because each opening creates a reliability problem. In the case of brazing and soldering, the seal is reheated and separated, which causes oxidation to occur on the two mating surfaces. Care must be taken to remove the flux used to reduce this oxide in resealing, as it is readily trapped in the filler metal which can and has caused leaks in various systems, as shown in the typical x-ray of Fig. 24.2.

Typical designs for brazed or soldered joints in tubes and pipes are shown in Fig. 24.3. It is doubtful that brazing can be successfully used in separable seal applications because of the oxidation and diffusion problems encountered in reheating (1100 to 1900°F). Soldering, on the other hand, can be and has been employed in low temperature applications. The increase in strength of solders at very low temperatures (Ref. 3) can be noted on Fig. 24.4, which shows two typical solders and their mechanical behavior at various temperatures.

52

FIGURE 24.2 X-Ray of Soldered Copper Flange Joint

This full-size x-ray photograph, looking in the direction of flow,
shows several voids (light areas) that are largely filled with flux
from the soldering operation. In this application, a water line in-
tended for "infinite" life, the joint leaked after 3764 hours of service.
With improved soldering techniques and increased attention to removal
of flux, the joint was made leak-tight. For satisfactory leak-tightness,
the void area must be made less than 15% of the total flange area.
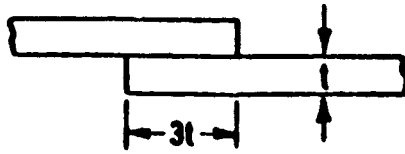
Lap Joint with Minimum Lap

Possible Locations of Alloy Rings

Use Only One

Possible Locations of Alloy Rings
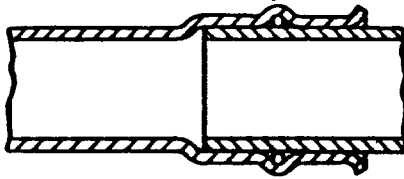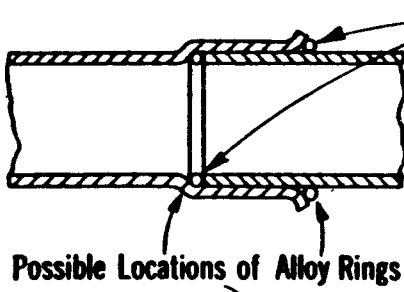
Well Designed Tubular Joints
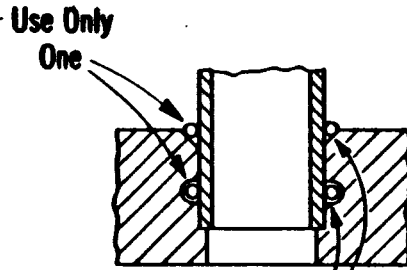
Good Tube to Tube Sheet Designs

Fig. 24.3 Typical Designs for Brazed or Soldered
Tube Joints

54

24-7
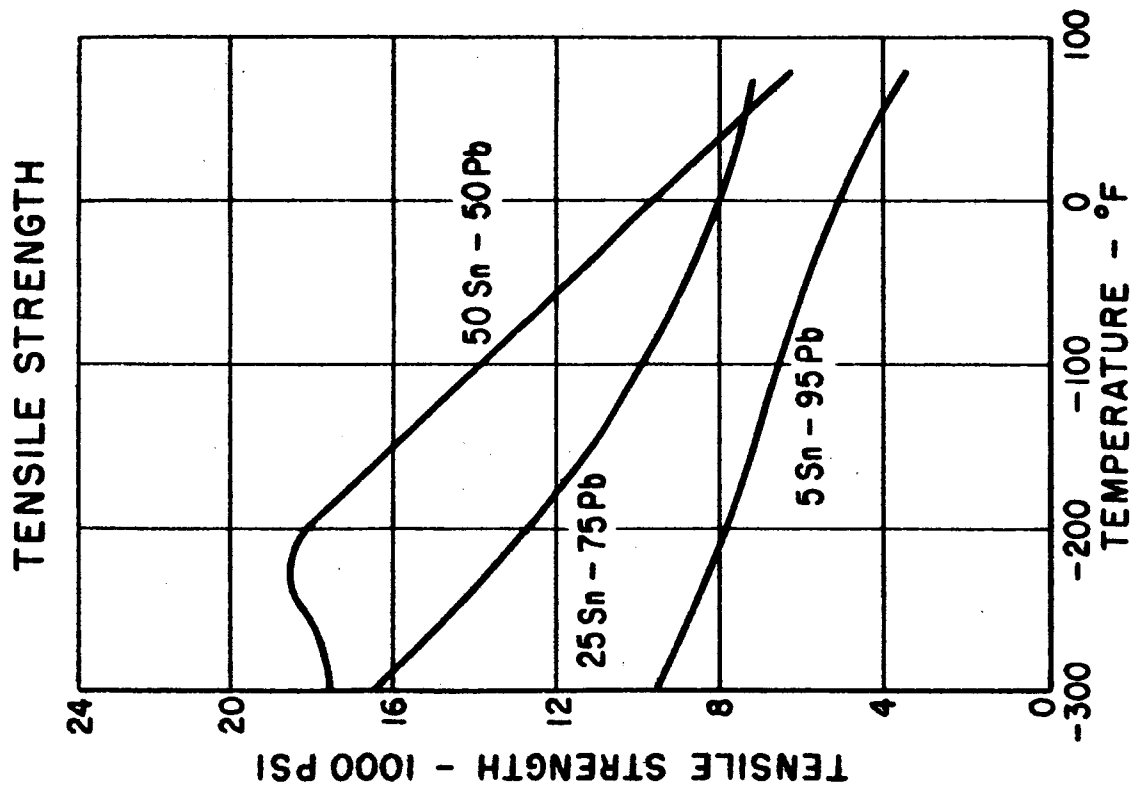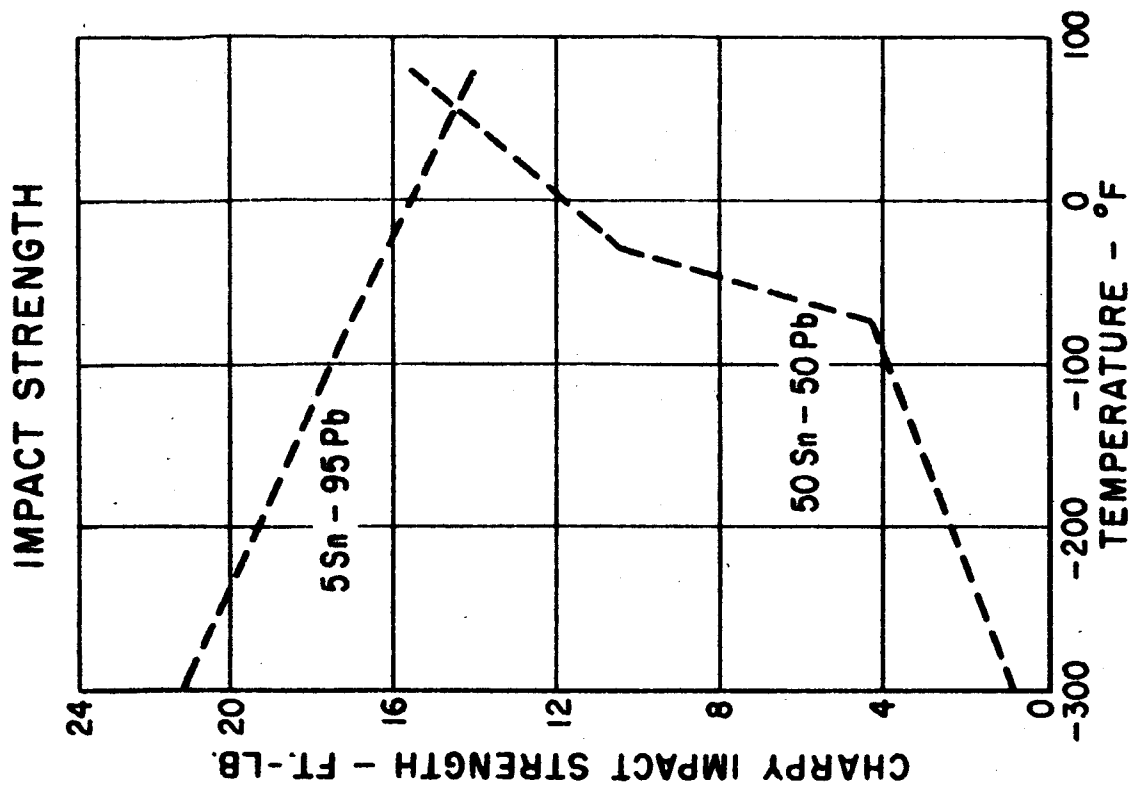
FIG. 24.4   Strength of Solders at Low Temperatures (Ref. 3)

24.4   Swaging(Cold Welding)

It is well known that when metal surfaces are pressed together, the oxide film will fragment if sufficient force is applied. When the high spots touch, the metal behind them suffers plastic deformation. However, oxides are brittle, and the oxide layer must fragment to conform to the changed surface contours. Because of this fragmentation, some metal-to-metal contact occurs which acts as true metallurgical bonds at these sites. An excellent illustration of this characteristic is seen when fresh surfaces of lead or very soft indium are twisted together and the resulting weld has a macro strength approaching that of the base metal. Any metal can be made to weld measurably by shearing the two surfaces together at sufficiently high pressure. However, the results are difficult to produce consistently.

Techniques for achieving consistently satisfactory pressure welds at room temperature were developed for aluminum and copper. These are embodied in the Koldweld[*] process. These techniques require as much as 33 per cent reduction in aluminum to obtain the desired metallurgical bond. These seals would not be reusable. In the case of tubes and pipes, a new mechanical seal (not metallurgical) called Swagelok[**] has been developed which provides a leak-tight seal at three points on the tube by slightly deforming the tube itself. These seals are excellent for applications not requiring wide temperature cycling. However, it is doubtful that they would meet either the high or low cycling applications being considered here.

---

[*]Koldweld Corporation, New York, New York

[**]Swagelok, Crawford Fitting Co., 884 East 140th St., Cleveland, Ohio

56

24.5 Conclusions

1. Each application will require a specific theoretical study of permeation rates once the materials and processes are established for the given system.

2. The inert arc welding of vacuum-tight tubes and pipes of aluminum and stainless steel are well established processes for one-time sealing applications. Reusable welded designs as outlined in this report have been made, although they have not been widely tested in the welding industry as of this date; however, welding is the only process capable of handling both high and low temperature applications.

3. Brazing can be successfully accomplished for applications in the range of room temperature to $1000^{\circ}F$. Data on brazed junction performance at $-450^{\circ}F$ are not readily available. The use of brazing in reusable seals will at best be very difficult to develop, and reliability will be in question due to excessive diffusion and oxidation problems on reheating.

4. Soldering has been successfully used in room temperature to $-450^{\circ}F$ applications. The choice of solder and method of perfecting the junctions will be dictated by the specific application. The higher temperature applications cannot be accomplished with solder seals.

5. Swaging (cold welding) could possibly be used in applications utilizing aluminum as the base material. It is not likely that these seals could be reused. No mechanical seal will meet the wide temperature ranges involved in these applications, due to relaxation and oxidation of the different members during its life.

6. In joints properly made by any of these processes, the leakage should be no greater than the permeation through the base metal.

57

24.6 <u>References</u>

1. D. P. Smith, <u>Hydrogen in Metals</u>, Chicago, University of Chicago Press, 1948, pp. 5,6.

2. American Welding Society, <u>Welding Handbook,</u> Fourth Edition, New York, 1958, Section 2, Chapter 27.

3. A. B. Kaufman, "Selecting Solders for Low-Temperature Service," <u>Materials in Design Engineering,</u> November 1958.

58

<u>DISTRIBUTION LIST FOR REPORTS ON CONTRACT NAS 8-4012</u>

<u>NASA Headquarters, Washington 25, D.C.</u>

Mr. Henry Burlage, Jr.
Chief, Liquid Propulsion Systems, RPL (3)

Mr. A.O. Tischler
Assistant Director for Propulsion, MLP (1)

<u>NASA, Marshall Space Flight Center, Huntsville, Alabama</u>

Mr. Charles Wood (M-P&VE-PT), Technical Manager (24)
Office of Technical Information, M-MS-IPC
Contracting Officer, M-P&C-C
Patent Office, M-PAT

<u>NASA Other Locations</u>

Technical & Scientific Information Facility
Attention: NASA Representative, Code CRT
P.O. Box 5700, Bethesda, Maryland   (24)

<u>Attention: Technical Librarian</u>

Ames Research Center
Moffett Field, California (2)

Goddard Space Flight Center
Greenbelt, Maryland   (2)

Jet Propulsion Laboratory
California Institute of Technology
4800 Oak Grove Drive
Pasadena, California   (2)

Langley Research Center
Langley Field, Virginia   (2)

Lewis Research Center
21000 Brookpark Road
Cleveland 35, Ohio   (2)

Marshall Space Flight Center
Huntsville, Alabama   (2)

Manned Spacecraft Center
Houston, Texas   (2)

Advanced Research Projects Agency
Pentagon, Room 3D154
Washington 25, D.C.

Aeronautical Systems Division
Air Force Systems Command
Wright-Patterson Air Force Base, Ohio

<u>Attention: Technical Librarian</u>

Air Force Missile Development Center
Holloman Air Force Base, New Mexico

Air Force Missile Test Center
Patrick Air Force Base, Florida

Air Force Systems Command, Dyna-Soar
Air Force Unit Post Office
Los Angeles 45, California

Army Ordnance Missile Command
Redstone Arsenal, Alabama

Armed Services Technical Information Agency
Arlington Hall Station
Arlington 12, Virginia

Arnold Engineering Development Center
A.E.O.R.
Tullahoma, Tennessee

Bureau of Naval Weapons
Department of the Navy
Washington 25, D.C.

Central Intelligence Agency
2430 E. Street, N.W.
Washington 25, D.C.

Headquarters, United States Air Force
Washington 25, D.C.

Office of Naval Research
Washington 25, D.C.

Attention: Technical Librarian

Picatinny Arsenal
Dover, New Jersey

Rocket Research Laboratories
Edwards Air Force Base, California

U.S. Naval Ordnance Test Station
China Lake, California

U.S. Atomic Energy Commission
Technical Information Services
Box 62
Oak Ridge, Tennessee

Liquid Propellant Information Agency
Johns Hopkins University
Applied Physics Laboratory
8621 Georgia Avenue
Silver Spring, Maryland

Aerojet-General Corporation
P.O. Box 296
Azusa, California

Aerojet-General Corporation
P. O. Box 1947
Sacramento 9, California

Aeronutronic
A Division of Ford Motor Company
Ford Road
Newport Beach, California

Aerospace Corporation
2400 East El Segundo Boulevard
El Segundo, California

Arthur D. Little, Inc.
Acorn Park
Cambridge 40, Massachusetts

Astropower, Inc., Subsidiary of Douglas
    Aircraft Company, Inc.
2968 Randolph Avenue
Costa Mesa, California

Astrosystems, Inc.
82 Naylon Avenue
Livingston, New Jersey

Atlantic Research Corporation
Edsall Road and Shirley Highway
Alexandria, Virginia

Attention: Technical Librarian

Beech Aircraft Corporation
Boulder Facility
Box 631
Boulder, Colorado

Bell Aerosystems Company
P. O. Box 1
Buffalo 5, New York

Bendix Systems Division
Bendix Corporation
Ann Arbor, Michigan

Boeing Company
P. O. Box 3707
Seattle 24, Washington

Convair (Astronautics)
Division of General Dynamics Corporation
P. O. Box 2672
San Diego 12, California

Curtiss-Wright Corporation
Wright Aeronautical Division
Wood-ridge, New Jersey

Douglas Aircraft Company, Inc.
Missile and Space Systems Division
3000 Ocean Park Boulevard
Santa Monica, California

Fairchild Stratos Corporation
Aircraft Missiles Division
Hagerstown, Maryland

General Electric Company
Missile and Space Vehicle Department
Box 8555
Philadelphia, Pennsylvania

General Electric Company
Rocket Propulsion Units
Building 300
Cincinnati 15, Ohio

Grumman Aircraft Engineering Corporation
Bethpage, Long Island, New York

Kidde Aero-Space Division
Walter Kidde and Company, Inc.
675 Main Street
Belleville 9, New Jersey

Attention: Technical Librarian

Lockheed Aircraft Corporation
Missile and Space Division
Sunnyvale, California

Lockheed Propulsion Company
P.O. Box 111
Redlands, California

Marquardt Corporation
16555 Saticoy Street
Box 2013 - South Annex
Van Nuys, California

Martin Division
Martin Marietta Corporation
Baltimore 3, Maryland

Martin Denver Division
Martin Marietta Corporation
Denver, Colorado

McDonnell Aircraft Corporation
P. O. Box 6101
Lambert Field, Missouri

North American Aviation, Inc.
Space & Information Systems Division
Downey, California

Northrup Corporation
1001 East Broadway
Hawthorne, California

Pratt & Whitney Aircraft Corporation
Florida Research & Development Center
West Palm Beach, Florida

Radio Corporation of America
Astro-Electronics Division
Defense Electronic Products
Princeton, New Jersey

Reaction Motors Division
Thiokol Chemical Corporation
Denville, New Jersey

Republic Aviation Corporation
Farmingdale
Long Island, New York

Attention: Technical Librarian

Rocketdyne (Library Dept. 586-306)
Division of North American Aviation, Inc.
6633 Canoga Avenue
Canoga Park, California

Space General Corporation
9200 Flair Avenue
El Monte, California

Space Technology Laboratories
P. O. Box 95001
Airport Station
Los Angeles 45, California

Stanford Research Institute
333 Ravenswood Avenue
Menlo Park, California

TAPCO Division
Thompson-Ramo-Wooldridge, Inc.
23555 Euclid Avenue
Cleveland 17, Ohio

Thiokol Chemical Corporation
Redstone Division
Huntsville, Alabama

United Aircraft Corporation
East Hartford Plant
400 Main Street
Hartford, Connecticut

United Technology Corporation
587 Methilda Avenue
Sunnyvale, California

Vought Astronautics
Box 5907
Dallas 22, Texas

Armour Research Foundation
Illinois Institute of Technology
10 West 35th Street
Chicago 16, Illinois

Battelle Memorial Institute
505 King Avenue
Columbus 1, Ohio

National Bureau of Standards
Cryogenic Engineering Laboratory
Boulder, Colorado